Title

Cytomegalovirus Impairs Cytotrophoblast-Induced Lymphangiogenesis and Vascular Remodeling in an in Vivo Human Placentation Model

Journal

American Journal Of Pathology, 181(5)

ISSN

0002-9440

Authors

Tabata, Takako
Petitt, Matthew
Fang-Hoover, June
et al.

Publication Date

2012-11-01

DOI

10.1016/j.ajpath.2012.08.003

Peer reviewed

The American Journal of Pathology, Vol. 181, No. 5, November 2012

http://dx.doi.org/10.1016/j.ajpath.2012.08.003

Animal Models

Cytomegalovirus Impairs Cytotrophoblast-Induced Lymphangiogenesis and Vascular Remodeling in an *in Vivo* Human Placentation Model

Takako Tabata,* Matthew Petitt,* June Fang-Hoover,* Jose Rivera,† Naoki Nozawa,‡ Stephen Shiboski,§ Naoki Inoue,‡ and Lenore Pereira*

From the Department of Cell and Tissue Biology, School of Dentistry, the Division of Experimental Medicine,† Department of Medicine, San Francisco General Hospital, and the Department of Epidemiology and Biostatistics,§ School of Medicine, University of California, San Francisco, San Francisco, California; and the National Institutes of Infectious Diseases,‡ Tokyo, Japan*

We investigated human cytomegalovirus pathogenesis by comparing infection with the low-passage, endotheliotropic strain VR1814 and the attenuated laboratory strain AD169 in human placental villi as explants *in vitro* and xenografts transplanted into kidney capsules of SCID mice (ie, mice with severe combined immunodeficiency). In this *in vivo* human placentation model, human cytotrophoblasts invade the renal parenchyma, remodel resident arteries, and induce a robust lymphangiogenic response. VR1814 replicated in villous and cell column cytotrophoblasts and reduced formation of anchoring villi *in vitro*. In xenografts, infected cytotrophoblasts had a severely diminished capacity to invade and remodel resident arteries. Infiltrating lymphatic endothelial cells proliferated, aggregated, and failed to form lymphatic vessels. In contrast, AD169 grew poorly in cytotrophoblasts in explants, and anchoring villi formed normally *in vitro*. Likewise, viral replication was impaired in xenografts, and cytotrophoblasts retained invasive capacity, but some partially remodeled blood vessels incorporated lymphatic endothelial cells and were permeable to blood. The expression of both vascular endothelial growth factor (VEGF)-C and basic fibroblast growth factor increased in VR1814-infected explants, whereas VEGF-A and soluble VEGF receptor-3 increased in those infected with AD169. Our results suggest that viral replication and paracrine factors could undermine vascular remodeling and cytotrophoblast-induced lymphangiogenesis, contributing to bleeding, hypoxia, and edema in pregnancies complicated by congenital human cytomegalovirus infection. *(Am J Pathol 2012, 181:1540–1559; http://dx.doi.org/10.1016/j.ajpath.2012.08.003)*

Human cytomegalovirus (HCMV) is the leading cause of congenital viral infection, with an incidence in the United States of approximately 1% to 3% of live births.[1] Primary maternal HCMV infection during gestation poses a 40% to 50% risk of intrauterine transmission, whereas recurrent infection in seropositive mothers rarely causes disease.[2,3] Symptomatic infants (25%) have intrauterine growth restriction (IUGR) and permanent birth defects, including neurological deficiencies, retinopathy, and sensorineuronal deafness.[4–6] Congenital disease is more severe when primary maternal infection occurs in the first trimester.[7] IUGR and spontaneous abortion in the absence of fetal HCMV infection can result from placental pathology.[8–10] Placentas infected in early gestation show long-standing damage and fibrosis at the uterine-placental interface, which impairs critical functions and results in a hypoxic intrauterine environment.[10–15] Despite the prevalence and the medical and societal impact of congenital HCMV infection, the mechanisms of virus replication, pathogenesis, and transplacental transmission are still unresolved because of the complex nature of placental development and extreme species specificity of HCMV, which replicates only in human tissues.

Differentiating/invading cytotrophoblasts switch to an endothelial phenotype in a process that is similar to vas-

Supported by grants from the NIH (R21 AI090200, R01 AI046657, and R56 AI073753 to L.P.; R21 HD061890 to T.T.), grants from the International Aids Vaccine Initiative UCALIFRSA1002 (L.P.), Japan Research Fund SHC4401 (N.I.), and a Scholarship Award in Herpesvirus Research from the Japan Herpesvirus Infections Forum (N.N.).

Accepted for publication August 1, 2012.

Current address of N.N., Drug Discovery Research Laboratories, Maruho Co, LTD, Kyoto, Japan.

Address reprint requests to Lenore Pereira, Ph.D., University of California, San Francisco, 513 Parnassus Ave, San Francisco, CA 94143-0640. E-mail: lenore.pereira@ucsf.edu.

culogenesis.[16] The cells up-regulate novel adhesion molecules and proteinases that enable their attachment to and invasion of the uterus. Interstitial invasion requires down-regulation of integrins characteristic of epithelial cells and novel expression of the integrins $\alpha1\beta1$, $\alpha5\beta1$, and $\alpha v\beta3$.[17] Endovascular cytotrophoblasts that remodel uterine blood vessels transform their adhesion receptor phenotype to resemble that of endothelial cells, expressing vascular-endothelial cadherin, platelet-endothelial adhesion molecule-1, and vascular endothelial adhesion molecule-1.[16,18] Like endothelial cells, cytotrophoblasts express substances that influence vasculogenesis and angiogenesis, including the vascular endothelial growth factor (VEGF) family ligands VEGF-A and VEGF-C and receptors VEGFR-1 [fms-like tyrosine kinase 1 (Flt-1)] and VEGFR-3.[19–21] Expression of these molecules changes as the cells differentiate/invade, and they regulate cytotrophoblast survival in the remodeled uterine vasculature. Finally, as hemiallogeneic embryonic/fetal cells, invasive cytotrophoblasts must avoid maternal immune responses. Their expression of the nonclassical major histocompatibility complex (MHC) class I molecules HLA-G[22,23] and HLA-C, which have limited polymorphisms,[24,25] contributes to their lack of immunogenicity.

Previous studies led to a rudimentary understanding of HCMV infection of the human placenta and identified several molecular mechanisms that impair functions of differentiating/invading cytotrophoblasts. HCMV infection dysregulates the expression of key integrins required for cell invasiveness,[26,27] reduces the expression of matrix metalloproteinase-9,[27] and down-regulates cell-cell and cell-matrix adhesion molecules,[28] including those required for pseudovasculogenesis[16] and vascular remodeling.[18] The immunosuppressive viral cytokine cmv IL-10 further reduces cytotrophoblast invasion through paracrine effects that increase IL-10 expression.[27,28] Peroxisome proliferator-activated receptor γ activation by infection also compromises cytotrophoblast functions.[29,30] In chorionic villi, the neonatal Fc receptor for IgG, expressed in syncytiotrophoblasts that contact maternal blood, transcytoses circulating maternal antibodies.[31–33] In conjunction with neutralizing titers, developmental expression of HCMV receptors, EGFR, and integrins[34–37] determines susceptibility to infection.[33,38–40] HCMV infects spatially distinct populations of cytotrophoblasts that express $\alpha1\beta1$ and $\alpha v\beta3$ integrins used as surface receptors.[41]

How HCMV disseminates to the placenta and the early stages of pathogenesis in pregnancy are still unresolved because of the virus' extreme host range restriction. A successful approach to overcome the obstacle to studies of HCMV *in vivo* has been to infect SCID mice (ie, mice with severe combined immunodeficiency) that have received xenografts of human tissues. Infection of human fetal thymus/liver under the mouse kidney capsule showed that medullary epithelial cells are prominent targets of HCMV replication.[42] Thus, dramatic interstrain differences were evident in replication of low-passage clinical isolates and laboratory strains in thymus/liver xenografts *in vivo*.[42,43] The strain Toledo replicates to high titers in implants, whereas the laboratory strains AD169 and Towne, serially passaged in fibroblasts, are attenuated and fail to propagate in tissues *in vivo*.[43] AD169 lacks a 15-kb segment of viral genome that encodes at least 19 open reading frames present in the genomes of all pathogenic clinical strains.[44] A deletion mutant of Toledo lacking these sequences, although exhibiting only a minor growth defect in fibroblasts, fails to replicate in thymus/liver implants in SCID mice, evidence that genes in this region are central to infection *in vivo*.[45] HCMV replication in endothelial and epithelial cells correlates with determinants specified by ORFs UL128-131A,[46,47] which are highly conserved in clinical isolates[48] and which elicit neutralizing antibodies in humans.[49,50]

Herein, we investigated HCMV pathogenesis in infected human placental villous explants and in xenografts maintained *in vivo*. We used a model of human placentation to investigate the vascular effects of fetal cytotrophoblasts in human placental villi transplanted beneath the kidney capsules of SCID mice.[21] VR1814, a clinical isolate, infected cell column cytotrophoblasts in placental explants and impaired the formation of anchoring villi *in vitro*. In xenografts, VR1814-infected placental cells had a severely diminished capacity to invade and form lymphatic vessels. In striking contrast, AD169 replicated poorly in villous explants. In SCID mice, AD169-infected cytotrophoblasts remodeled the resident arteries, but these were faulty. Our results show, for the first time to our knowledge, that *HCMV* genes dispensable for growth in culture function as determinants of pathogenesis that could contribute to vascular anomalies that originate in early placentation.

Materials and Methods

Human Placental Villous Explants, Culture, and HCMV Infection in Vitro

Approval for this project was obtained from the Institutional Review Board at the University of California, San Francisco. Protocols involving human fetal and placental tissue from deliveries at Moffitt Hospital (San Francisco, CA) and use of animals were approved by the Committees on Human and Animal Research, respectively. Normal human placentas ($n = 3$) were obtained from elective termination of pregnancy (Advanced Bioscience Resources, Alameda, CA). Procedures for preparation of organ cultures (explants) of human placental villi were reported.[26] Briefly, chorionic villi dissected from placentas at 6 to 8 weeks' gestational age were cultured on Millicell-CM inserts (0.4-μm pore size; Millipore, Billerica, MA) coated with Matrigel (BD Biosciences, Bedford, MA) in explant medium: Dulbecco's modified Eagle's medium/F12 (1:1) (Gibco, Carlsbad, CA) with 10% Hyclone fetal bovine serum (FBS; Thermo Scientific, South Logan, UT), 1% penicillin-streptomycin, and 1% amino acid. After 18 to 20 hours, explants were infected [2×10^6 plaque-forming units (PFU) per explant] with HCMV VR1814, a clinical isolate maintained at low passage and propagated in human umbilical vein endothelial cells,[51] or AD169, a laboratory strain serially passaged in human

foreskin fibroblasts. Explants were maintained for 3 days after infection and fixed in 4% paraformaldehyde (Wako Chemical USA, Richmond, VA) for histological analysis.

Primary Cytotrophoblast Isolation, Culture, and HCMV Infection in Vitro

Cells were isolated from second-trimester human placentas by previously described methods.[26,52] Briefly, placentas were subjected to a series of enzymatic digestions, which detached cytotrophoblast progenitors from the stromal cores of the chorionic villi. Cells were then purified over a Percoll gradient, cultured on substrates coated with Matrigel, and plated in serum-free medium: Dulbecco's modified Eagle's medium/F12 (1:1), with 2% Nutridoma (Roche Diagnostics, Indianapolis, IN), 1% sodium pyruvate, 1% HEPES, 1% penicillin-streptomycin, and 0.1% gentamicin (UCSF Cell Culture Facility, San Francisco, CA).[26,52] After 16 hours, cytotrophoblasts were infected with AD169 or VR1814 at a multiplicity of infection of 2 and maintained for 3 days.[27]

In Vivo *Transplantation of Human Placental Villi and HCMV Infection in SCID Mice*

Homozygous C.B-17 *scid/scid* mice (Taconic, Germantown, NY) were the recipients of human chorionic villi (placentas at 8 to 10 weeks' gestation). *In toto*, chorionic villi dissected from five first-trimester placentas were transplanted to 65 SCID mice. To determine the optimal time point for HCMV infection, based on recovery of infectious progeny, placental villi were infected immediately before transplantation ($n = 30$ mice) or after 3 weeks *in vivo* ($n = 22$ mice). Mock-infected controls ($n = 6$ mice) were maintained *in vivo* for the intervals determined by the experimental conditions, and titration indicated the controls were virus free. Dissected placental villi were washed with serum-free medium, infected with VR1814 (1×10^6 PFU) for 1 hour, transplanted under the kidney capsular membrane using surgical methods, and maintained for 3 weeks after infection *in vivo*.[21,53] Alternatively, placental villi were first transplanted and maintained *in vivo* for 4 weeks. At that time, implants were surgically exposed, injected with virus (100 μL, 1×10^6 PFU), and maintained *in vivo* an additional 3 weeks. To study the capacity of virulent and attenuated HCMV strains to grow *in vivo*, placental villi were cultured for 18 to 20 hours on Matrigel, infected with VR1814 or AD169 (2×10^6 PFU), transplanted into SCID mice ($n = 32$ mice), and maintained for 3 weeks. Virus titers used to infect villous explants and xenografts were determined empirically (data not shown). Mock-infected control placental villi were virus free. Mice were housed under pathogen-free conditions and sacrificed, and kidneys with implants were recovered. One half of the kidney implant was immediately fixed in 4% paraformaldehyde at 4°C for histological analysis, and the other half was snap frozen and stored at −80°C for titration of progeny.

HCMV Titration in Placental Villous Implants in Vivo *Maintained in SCID Mice*

Frozen implants were sonicated in 0.5 mL cold Dulbecco's modified Eagle's medium containing 1% FBS on ice. Virus titers were determined by serial dilution of tissue homogenates, followed by rapid infectivity assays on human foreskin fibroblast monolayers in duplicate.[26] Virus titers were expressed as $\log_{10}$ PFU/g protein of tissue homogenates.

Immunohistochemistry

Placental villous explants cultured on Matrigel *in vitro* and implants from SCID mice were fixed in 4% paraformaldehyde for 30 minutes and 3 to 6 hours, respectively, followed by sucrose gradients and embedded in gelatin or optimal cutting temperature compound, respectively. Decidual and placental biopsy specimens were also fixed and embedded in optimal cutting temperature compound. The tissues were frozen in dry ice and cut into sections (5 μm thick). For double immunostaining, tissue sections were simultaneously incubated with primary antibodies from various species and detected with fluorescein isothiocyanate– or tetramethyl rhodamine isothiocyanate–conjugated secondary antibodies (Jackson ImmunoResearch, West Grove, PA). Nuclei were counterstained with DAPI (Vector Laboratories, Burlingame, CA). Mouse monoclonal antibodies to HCMV immediate-early (IE 1&2) nuclear proteins (CH160) and glycoprotein B (gB) were produced in the Pereira Lab.[54,55] Rat monoclonal anti-human cytokeratin (clone 7D3) was a generous gift from Dr. Susan Fisher (University of California, San Francisco, San Francisco, CA). Mouse monoclonal anti-human HLA-G (clone 4H84) was a gift from Dr. Michael McMaster (University of California, San Francisco).[23] Rabbit polyclonal anti-integrin $\alpha 9\beta 1$ was a generous gift from Dr. Dean Sheppard (University of California, San Francisco).[56] Guinea pig anti-HCMV gB was a gift from Chiron Corporation (Emeryville, CA). The following antibodies were obtained from the companies listed: rabbit monoclonal anti-human/mouse Ki-67 (clone EPR3611; Abcam, Cambridge, MA), mouse monoclonal anti-human cytokeratin 7 (clone OV-TL 12/30; Dako, Carpentaria, CA), rabbit polyclonal anti-mouse lymphatic vessel endothelial hyaluronan receptor (LYVE-1; Fitzgerald Industries International, North Acton, MA), rabbit polyclonal anti-human VEGF-A (A-20) and rabbit polyclonal anti-ephrin B2 (P-20) (Santa Cruz Biotechnology, Santa Cruz, CA), goat polyclonal anti-human VEGF-C and goat polyclonal anti-carcinoembryonic antigen-related cell adhesion molecule 1 (CEACAM1)/CD66a (R&D Systems, Minneapolis, MN), rat monoclonal anti-mouse CD31 (clone MEC13.3; BD Pharmingen, San Diego, CA), and Syrian hamster monoclonal anti-mouse podoplanin (Abcam). Apoptosis was detected by TUNEL using the *In Situ* Cell Death Detection Kit, Fluorescein (Roche Applied Science, Indianapolis, IN).

Measurements of Anchoring Villi Formed in Placental Explants in Vitro

Sizes of anchoring villi formed in uninfected controls and HCMV-infected explants at 3 days after infection were quantified by measuring the areas of explant outgrowths from anchoring villi visible in digital photographs. Explants were photographed by phase-contrast microscopy on a Nikon Eclipse TE2000-S microscope (Nikon Instruments, Melville, NY) equipped with a Kodak DC215 digital camera (Eastman Kodak, Rochester, NY) using a ×4 objective (×40 total magnification). All digital images were of the same magnification, dimensions, and pixel densities. Areas were measured by importing images into Adobe Photoshop CS5.1 (Adobe Systems Inc., San Jose, CA), outlining the visible areas of outgrowth from the villi with the lasso tool, and recording the number of pixels within the outlined areas from the histogram function (at cache level 1). Numbers of villi examined are as follows: mock-infected, $n = 25$; AD169, $n = 21$; and VR1814, $n = 43$.

Quantification of Cytotrophoblast Interstitial Invasion into Renal Parenchyma

A total of 15 to 30 sections were prepared from each placental villous implant in kidneys of SCID mice. Two centrally located sections were stained with H&E. For each implant, one entire H&E-stained section was digitally photographed by light microscopy using a ×4 objective lens (×40 total magnification) on a Nikon Eclipse 50i microscope equipped with a SPOT 7.4 Slider camera (Diagnostic Instruments, Sterling Heights, MI). A total of 10 to 20 adjacent images of an entire section were imported into Adobe Photoshop CS5.1 and merged using the automated photomerge function to generate an image of an entire implant in the kidney parenchyma. The degree of implant invasion (ie, cytotrophoblast-occupied kidney parenchyma) was measured by outlining implants with the lasso tool and recording the number of pixels outlined (at cache level 1). The total implant area, including the portion external to the kidney surface proper, was measured directly by outlining. The area of cytotrophoblast-occupied kidney parenchyma was determined by subtracting the external portion from the total area of the implant. Placental villous implants were defined in H&E-stained sections by their morphological characteristics, which are distinct from those of the kidney parenchyma. Adjacent sections were immunostained for cytokeratin to confirm the degree of invasion, including small clusters and individual cytotrophoblasts that projected deeper into the parenchyma than the main invasion front.

Quantification of Blood Vessel Sizes

To determine the relative sizes of remodeled blood vessels within implants, H&E-stained sections were photographed at ×40 magnification, and images were analyzed using Photoshop CS5.1. For each section, the cross-sectional areas of the five largest discernible vessels (ie, those that had clearly defined walls and, in most cases, erythrocytes) were measured by outlining with the lasso tool, determining the number of pixels encircled, and converting pixel area to standard area units (mm^2). Most VR1814-infected implants had few or no discernible blood vessels. Both average vessel size and total cross-sectional area of perfusion for these and other implants lacking discernible vessels were considered 0. To quantify vessel diameter, 26 vessels were measured in six AD169-infected implants. For many AD169-infected and control implants, there were no clear distinctions between large vessels; rather, they appeared to contain networks of interconnected vessels. The results are expressed as the average total cross-sectional area of the five largest discernible vessels in each section, rather than average individual vessel size, because total area more accurately represents the differences between conditions. In most cases, the five largest vessels accounted for all clearly discernible large vessels and, thus, represented a good approximation of the total vessel area within the implant.

Quantification of Lymphatic Endothelial Cell Proliferation in the Renal Parenchyma

Proliferation of mouse lymphatic endothelial cells was quantified by immunostaining with anti-Ki-67 and anti-mouse LYVE-1 antibodies. The staining images (×200 total magnification) were acquired using a Nikon Eclipse 50i microscope and further analyzed quantitatively using ImageJ software version 1.44o (NIH, Bethesda, MD) or Adobe Photoshop CS 5.1. The numbers of LYVE-1– and Ki-67–positive lymphatic endothelial cells per field were counted, and the proliferation index was expressed as a percentage of Ki-67–positive cells.

Quantification of Factors in Conditioned Media

Conditioned media from control and infected cytotrophoblasts and placental villous explants on Matrigel *in vitro* were collected at 1 and 3 days after infection, cleared by centrifugation, and stored at −80°C. Levels of lymphangiogenic factors and chemokines were quantified using a human VEGF-C enzyme-linked immunosorbent assay (ELISA) kit (Syd Labs, Malden, MA), basic fibroblast growth factor (bFGF), human IL-6 Quantikine ELISA kits, and the human VEGFR3 DuoSet ELISA Development System (R&D Systems). Bioactive VEGF-A was measured using human VEGF-A BioLISA (eBioscience, San Diego, CA).

Lymphatic Endothelial Cell Proliferation Assays

Lymphatic endothelial cell proliferation was measured by MTT cell proliferation assays.[57] Human lymphatic endothelial cells (HLECs) isolated from lymph nodes (ScienCell Research Laboratories, Carlsbad, CA) were plated on fibronectin-coated (1 mg/mL), 96-well plates (5×10^3 cells per well) in endothelial cell medium (ECM) supplemented with endothelial cell growth supplement and 5%

FBS (ScienCell Research Laboratories), referred to as growth factor medium (GFM), for 3 days, and then starved for 24 hours in ECM containing 0.5% FBS (control media). Media were then replaced with 100 μL of control media, with or without recombinant human VEGF-A, VEGF-C, or bFGF proteins (R&D Systems). ECM supplemented with endothelial cell growth supplement and 5% FBS (GFM) was used as a positive control. After 72 hours' incubation, 20 μL of MTT (5 mg/mL) solution was added to each well, and the plates were further incubated for 24 hours at 37°C. The media were then removed, 100 μL of dimethyl sulfoxide was added to each well to dissolve the blue crystals, and absorbance was measured at 562 nm with a reference filter of 650 nm.

To assess the effect of conditioned media from control and infected cytotrophoblasts on lymphatic endothelial cell proliferation, conditioned media from control and infected cells on Matrigel were collected at 2 days after infection. Starved HLECs were then cultured with a mixture of 50 μL of conditioned medium and 50 μL of control medium for 72 hours, and MTT assays were performed. As a control, we used a mixture (referred to as SF-C for serum free and control) of 50 μL of serum-free medium (as used for culturing cytotrophoblasts, previously described) and 50 μL of control medium. To assess the functional contributions of particular growth factors, cells were incubated with blocking antibodies (anti-bFGF, 5 μg/mL; R&D Systems) or recombinant human Fc chimeras (VEGFR-1/Flt-1 and VEGFR-3/Flt-4, 5 μg/mL; R&D Systems) for 30 minutes before the addition of conditioned media. Pilot studies were conducted to determine effective inhibitory concentrations; concentrations >5 μg/mL did not lead to significantly greater inhibition for any of the three inhibitors. Isotype control antibodies (goat IgG, 5 μg/mL; R&D Systems) and a recombinant human CD6–Fc chimera (5 μg/mL; R&D Systems) were used as controls.

In the figures, the degree of cell proliferation is expressed as percentage of control values (from cells cultured in control media). Experiments to assess the effect of growth factors and cytotrophoblast-conditioned media were performed at least six times. Results of blocking experiments are expressed as percentage of values obtained using conditioned media without inhibitors. Blocking experiments were performed at least three times. The significance of differences was determined using the Student's *t*-test.

Statistical Analysis

Average outcomes were compared between groups defined by time period or treatment type using rank-based Kruskal-Wallis tests. For replicate outcomes (measured more than once per individual sample), between-group comparisons were based on linear regression models for log-transformed outcomes, with robust variances accounting for possible within-individual correlation in outcomes. To assess the possible effect of nonnormal outcome distributions on results, we repeated regression analyses assuming γ-distributed outcomes. No major differences were noted, so only the original regression results are reported.

The relationship between viral titer and percentage of infected cytotrophoblasts was determined by the Spearman rank correlation coefficient. Statistical data analysis of the lymphatic proliferation index was performed using the Pearson's χ^2 test.

Box-and-whisker plots were generated in Microsoft Excel (Microsoft Inc., Redmond, WA) using standard Excel functions. All box-and-whisker plots were made by dividing data sets into four quartiles (ie, each representing 25% of the data points). The box represents the second and third quartiles, which are divided by the horizontal bar representing the median. The whiskers span the first quartile (from the second quartile box down to the minimum) and the fourth quartile (from the third quartile box up to the maximum). Any data not included between the whiskers were plotted as an outlier with a small circle. The Student's *t*-test was used to determine the significance of the difference in expression between control and HCMV infection. $P < 0.05$ was considered significant.

Institutional Approvals

Approval for this project was obtained from the Institutional Review Board at the University of California, San Francisco. Protocols involving human fetal and placental tissue from deliveries at Moffitt Hospital and use of animals were approved by the Committees on Human and Animal Research, respectively.

Results

The Pathogenic HCMV Strain VR1814 Infects Cytotrophoblasts in Placental Explants and Impairs Development in Vitro

In the first set of experiments, we infected placental villous explants with AD169 or VR1814 and compared the development of anchoring villi *in vitro*. Representative mock-infected controls and virus-infected explants are shown (Figure 1, A–F). The controls developed robust cell columns and anchoring villi with cytotrophoblasts that aggregated and attached the explants to the extracellular matrix substrate (Matrigel; Figure 1, A and D). Surprisingly, AD169-infected explants formed normal-sized anchoring villi indistinguishable from controls (Figure 1, B and E). In contrast, VR1814-infected explants formed spindly cell columns composed largely of individual cytotrophoblasts on top of the substrate (Figure 1, C and F). Analysis of cytotrophoblasts within the placental villi revealed that AD169 infected few cells and expressed IE1&2 proteins (Figure 1G). Occasional infected cells also expressed gB, suggesting that replication was restricted (data not shown). In contrast, many VR1814-infected cytotrophoblasts expressed IE1&2 (Figure 1, H and I) and gB (Figure 1J). Invasive cytotrophoblasts differentiated and expressed MHC class I HLA-G but were down-regulated in VR1814-infected cells expressing gB (Figure 1J), as previously reported.[26,28]

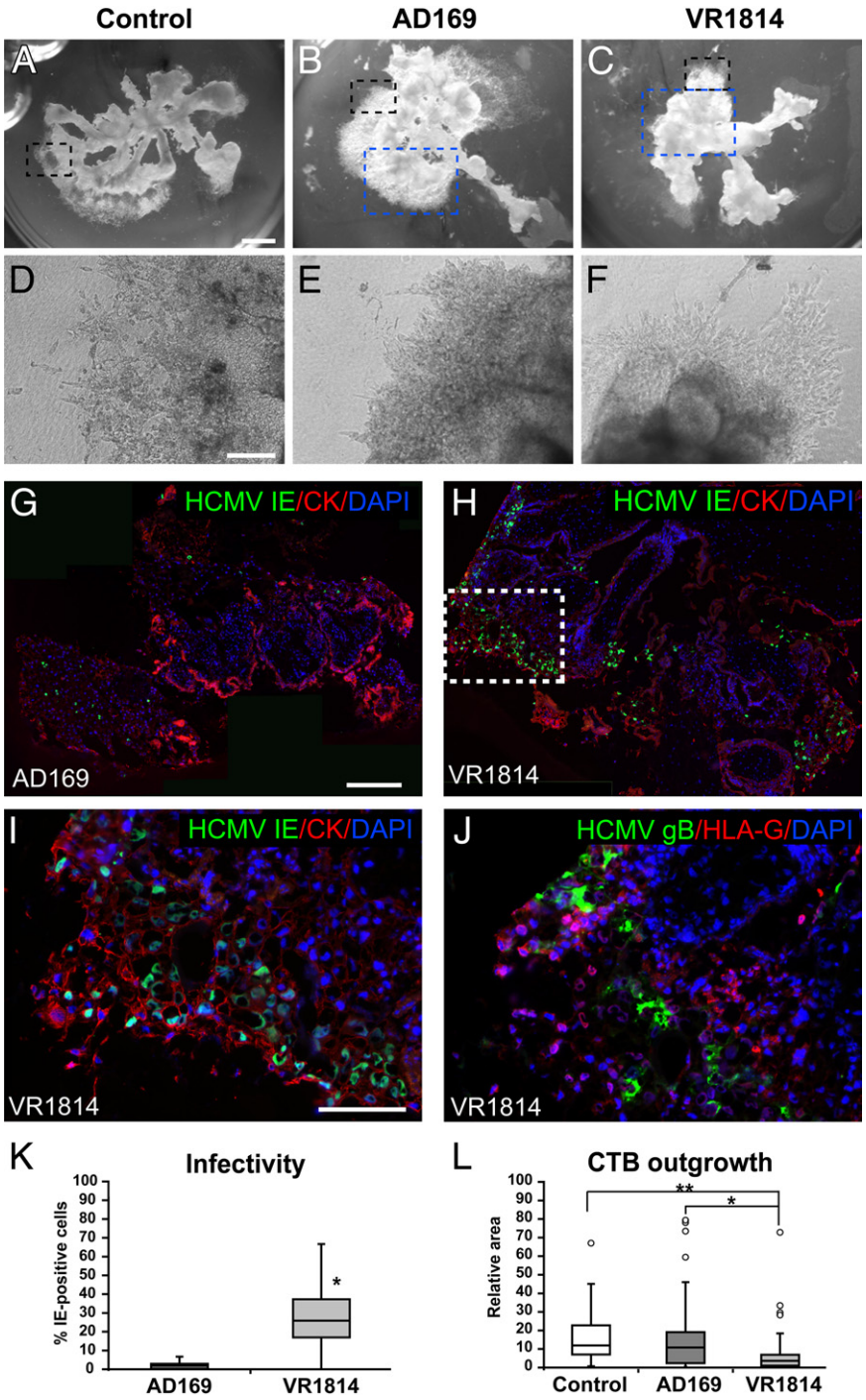

Figure 1. VR1814, a pathogenic HCMV strain, infects progenitor cytotrophoblasts in placental chorionic villous explants, reducing anchoring villous development. **A–C:** Villous explants with anchoring villi. Original magnification, ×2. **D–F:** Higher magnification of the areas marked by the **black dashed box** in **A–C**. Original magnification, ×100. **A** and **D:** Mock-infected controls. **B** and **E:** AD169 infection. **C** and **F:** VR1814 infection. Cytotrophoblasts are immunostained for expression of cytokeratin (CK) and HCMV IE1&2 in explants infected with AD169 (blue dashed box from **B**) (**G**) and VR1814 (**blue dashed box** from **C**) (**H**). Original magnification: ×40 (**H**); ×200 (**I**, enlargement of the boxed area in **H**.). **J:** The section adjacent to that in **I** is stained for HLA-G and gB. Original magnification, ×200. Nuclei are counterstained with DAPI. **K:** Number of AD169- and VR1814-infected cytotrophoblasts in cell columns: AD169 (explants, 5; cell columns, 19) and VR1814 (explants, 6; cell columns, 33). $^{*}P < 0.0001$ (Student's *t*-test). **L:** Measurements of anchoring villi of mock-infected control and AD169- and VR1814-infected explants: mock-infected control (explants, 7; counted villi, 25), AD169 (explants, 7; counted villi, 21), and VR1814 (explants, 16; counted villi, 43). $^{*}P < 0.001$, $^{**}P < 0.0001$ (Student's *t*-test). Scale bars: 1 mm (**A–C**); 200 μm (**D–F**); 200 μm (**G** and **H**); 100 μm (**I** and **J**).

Because AD169 and VR1814 exhibited markedly distinct levels of infection and gB expression in placental explants during a 3-day interval, too short for titration of viral replication, we quantified the differences by counting the number of cytotrophoblasts expressing IE1&2 proteins in the cell columns and anchoring villi (Figure 1K). AD169-infected explants contained a median of 2% infected cytotrophoblasts, with a 5% maximum. In contrast, VR1814-infected placental villi contained a median of 26% infected cells, with a 67% maximum. To quantify the effects on development of anchoring villi, we measured the sizes of villi formed by measuring the areas covered by the villous outgrowths at 3 days after infection (Figure 1L). Control and AD169-infected explants were comparable, with median sizes (excluding outliers; see *Materials and Methods*) of 12 and 11 relative units for control and AD169, respectively, and a maximum of approximately 45 relative units. In contrast, VR1814-infected explants formed significantly smaller villi, with a median size of 3.6 relative units (ie, <10% the size of those in control and AD169-infected explants) and a maximum of 18 relative units ($P < 0.0001$ compared with

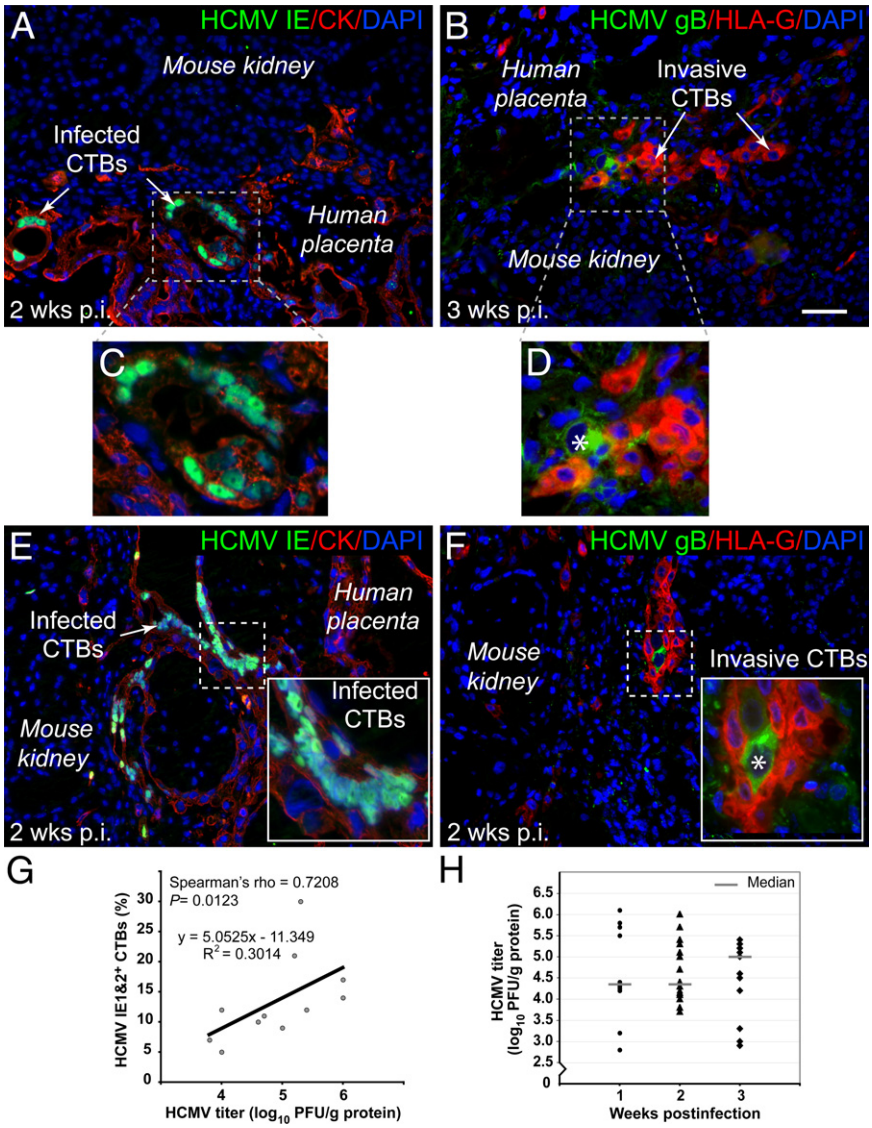

Figure 2. VR1814 replicates in cytotrophoblasts of human placental villi transplanted under the kidney capsules of SCID mice. **A** and **B:** Placental villi are infected before transplantation, with implants harvested at 2 and 3 weeks after infection. **C** and **D: Insets** from **A** and **B**. **E** and **F:** Placental villi are infected 4 weeks after transplantation, harvested at 2 weeks after infection. **A**, **C**, and **E:** Cytotrophoblasts are immunostained for expression of cytokeratin (CK) and HCMV IE1&2 proteins in infected cells. **B**, **D**, and **F:** Differentiating cytotrophoblasts are immunostained for expression of MHC class I HLA-G and HCMV gB in infected cells. **Asterisk** indicates gB expression in cytotrophoblasts. **G:** Correlation between number of infected cytotrophoblasts and titer of virus recovered from implants. The relationship between viral titer and percentage of cytotrophoblasts (CTBs) infected is determined by Spearman's rank correlation coefficient (n = 11). **H:** Titer of VR1814 recovered from homogenates of 39 villous implants in human fibroblasts at 3 weekly intervals after infection: 1 week (n = 10), 2 weeks (n = 16), and 3 weeks (n = 13). Scale bar = 50 μm.

control). Together, the results showed that VR1814 infected cell column cytotrophoblasts of placental explants and impaired functions of the subpopulation of cells that contribute to forming anchoring villi, reducing their size.

VR1814 Replicates in Cytotrophoblasts of Human Placental Villi Transplanted to SCID Mice

To study VR1814 replication in the tissue environment *in vivo*, human placental villi transplanted under the kidney capsules of SCID mice were subjected to infection. Conditions for optimal viral replication were determined, including infection before or after transplantation and the interval for maintenance of infected implants needed to recover maximal viral titers. Representative sections of placental villous implants, infected before transplantation and harvested at 2 weeks (Figure 2, A and C) and 3 weeks (Figure 2, B and D), are shown. Implants infected at 4 weeks and harvested 2 weeks after infection (total, 6 weeks *in vivo*) (Figure 2, E and F) are also shown. Under both conditions, cytotrophoblasts expressed cytokeratin (Figure 2, A, C, and E), and differentiating cells expressed HLA-G (Figure 2, B, D, and F). Viral replication was detected at 2 and 3 weeks after infection as discrete foci of infected cytotrophoblasts expressing IE1&2 proteins (Figure 2, A, C, and E) and gB (Figure 2, B, D, and F) among 10 to 20 placental cells. Typically, two or three foci of infected placental cells were observed in each section of VR1814-infected implants. Interestingly, VR1814-infected cytotrophoblasts that expressed gB down-regulated HLA-G *in vivo* (Figure 2, D and F), in accord with results from villous explants (Figure 1J).

Replication of VR1814 was quantified by counting the number of infected cytotrophoblasts and measuring the titer of virus recovered from homogenates of implants (Figure 2G). The number of infected cytotrophoblasts that expressed HCMV IE1&2 proteins in half of the implants correlated with the titer of virus recovered from the other

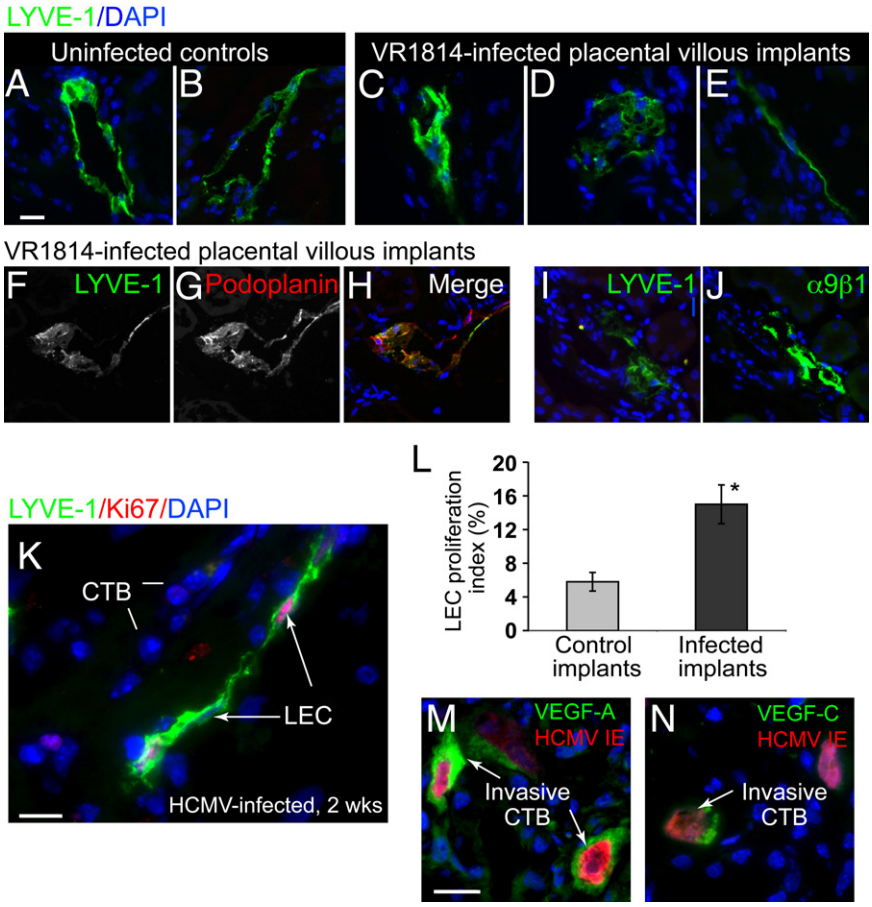

Figure 3. Aberrant lymphangiogenesis in VR1814-infected human placental villi *in vivo*. LYVE-1–immunostained lymphatic vessels and endothelial cells are shown. **A** and **B:** Normal vessels in mock-infected controls. **C–E:** Aberrant vessels in VR1814-infected placental implants. **F–H:** Co-immunostaining for LYVE-1 and podoplanin in VR1814-infected placental implants. **I** and **J:** Expression of LYVE-1 and integrin $\alpha 9\beta 1$ in adjacent sections of a VR1814-infected placental implant. **K:** Ki-67 immunostains proliferating LYVE-1–expressing lymphatic endothelial cells. **L:** Proliferation index of lymphatic endothelial cells in mock-infected controls and infected villi. The numbers of LYVE-1– and Ki-67–positive lymphatic endothelial cells per field are counted. The proliferation index is expressed as the percentage of LYVE-1–positive cells that are also Ki-67 positive. Control implants (n = 3, with 15 fields counted) and VR1814-infected implants (n = 9, with 27 fields counted) are shown. *P = 0.003 (Student's t-test). **M** and **N:** Immunostaining for VEGF-A (**M**) and VEGF-C (**N**) in implants. Scale bars: 20 μm (**A–J**); 5 μm (**K**); 5 μm (**M** and **N**). CTB, cytotrophoblast.

half (Spearman's ρ = 0.7208, P = 0.0123). Figure 2H shows the titer of virus recovered from VR1814-infected placental villous implants at 1, 2, and 3 weeks after infection (n = 39 mice). The results showed that VR1814 replicated in cytotrophoblasts in implants infected before or after transplantation into SCID mice. Titers of virus recovered from placental villi infected before transplantation ranged from 2.8 to 6.1 $\log_{10}$ PFU/g of protein. Likewise, titers recovered after direct inoculation of implants after transplantation ranged from 3.8 to 6.0 $\log_{10}$ PFU/g of protein. Median viral yields were 4.35 $\log_{10}$ PFU/g of protein at both 1 and 2 weeks after infection and 5.0 $\log_{10}$ PFU/g of protein at 3 weeks after infection. No significant difference in titers of virus recovered at different time points was found (Kruskal-Wallis equality-of-populations rank test). The finding that progeny virus recovered did not exceed the input amount indicated that HCMV infection was extremely limited in the tissue environment of the human placenta.

Dysregulated Lymphangiogenesis in VR1814-Infected Placental Implants in Vivo

In human placental villi maintained in SCID mouse kidney capsules, differentiating cytotrophoblasts induces infiltration of lymphatic endothelial cells, recapitulating a process that occurs during human placentation.[21] After having found that VR1814 replicates in human cytotrophoblasts maintained *in vivo* and alters their differentiation, we considered whether cytotrophoblast functions associated with lymphangiogenesis were also changed. To address this possibility, we studied the pattern of lymphatic vessels in the renal parenchyma transplanted with human placental villi at 3 weeks after infection with VR1814. Lymphatic endothelial cells were characterized by examining the expression of LYVE-1, a cell surface receptor on lymphatic endothelial cells. Mock-infected controls formed mostly intact lymphatic vessels with distinct lumens (Figure 3, A and B). In contrast, VR1814-infected implants had more aberrant forms, including partial lymphatic vessels, disorganized aggregates, and linear arrays of lymphatic endothelial cells (Figure 3, C–E). In the adult mouse kidney, LYVE-1 was expressed mainly in lymphatic endothelial cells and a subset of endothelial cells in the glomerular capillaries.[58] Thus, we examined the expression of two additional markers of lymphatic endothelial cells, podoplanin and integrin $\alpha 9\beta 1$, to confirm the identity of abnormal lymphatic endothelial cells in VR1814-infected villous explants. Double staining of LYVE-1 and podoplanin showed colocalization in vessel-like structures and amorphous cell clusters, although LYVE-1 staining in vessels was sometimes discontinuous at the vessel periphery, whereas podoplanin staining was not (Figure 3, F–H). Staining for

LYVE-1 and integrin $\alpha 9\beta 1$ in serial sections revealed their colocalization as well (Figure 3, I and J). These results indicated that both normal and aberrant vessel structures identified by LYVE-1 staining included lymphatic endothelial cells. A survey of infected placental implants ($n = 29$) suggested that the number of lymphatic endothelial cells was higher compared with controls. In sections immunostained for LYVE-1 and Ki-67 expression, a marker for cell proliferation, we identified a subpopulation of proliferating lymphatic endothelial cells (Figure 3K). Quantitative analysis indicated that approximately 14% of the cells were proliferating in infected implants, more than twice the number observed in mock-infected controls (6%), and the difference was significant ($P = 0.003$) (Figure 3L).

To determine whether VR1814 replication was associated with factors that induce lymphatic endothelial cell proliferation and migration *in vitro*,[21] implants were immunostained for VEGF-A and VEGF-C. In selected samples, we found that infected cytotrophoblasts expressing IE1&2 proteins strongly up-regulated expression of VEGF-A (Figure 3M) and VEGF-C (Figure 3N). Cytotrophoblasts in mock-infected implants failed to react by immunostaining, suggesting that expression was below the detection limit (data not shown). Together, the results of these experiments showed that some infected cytotrophoblasts up-regulate the production of lymphangiogenic factors that contribute to cell infiltration and proliferation and could alter vessel formation *in vivo*.

Reduced Interstitial and Endovascular Invasion by Cytotrophoblasts in VR1814-Infected Placental Implants

We reported that HCMV infection impairs the invasiveness of primary cytotrophoblasts *in vitro*.[26–28] In the present study, we showed that infection of placental villi with VR1814, but not infection with AD169, impaired the development of anchoring villi *in vitro* (Figure 1, C, F, and L). Based on these results, we theorized that infection could reduce interstitial invasiveness of cytotrophoblasts in the kidney parenchyma. To test this hypothesis, placental villi were infected with VR1814 or AD169 at 18 to 20 hours after attachment to Matrigel, then transplanted under the kidney capsules of SCID mice and maintained for 3 weeks. Representative implants immunostained for cytokeratin and CEACAM-1 (CD66a), a surface antigen expressed by invasive cytotrophoblasts,[59] showed the extent of the kidney parenchyma occupied by the placental cells (Figure 4). Mock-infected controls showed robust invasion (Figure 4, A–C). The cytotrophoblast-occupied area increased from the site of implantation shown at the left, and the invasion front extended well into the cortex, with select clusters migrating even more deeply (Figure 4, A–C). Interestingly, cytotrophoblast invasion was unchanged in AD169-infected implants, as expected from reduced infection *in vivo* (Figure 4, D–F). The placental cells invaded the kidney parenchyma, and the total area of invasion was comparable to controls (Figure 4, D–F). In contrast, cytotrophoblasts in VR1814-infected implants showed a strikingly reduced capacity for invasion in the renal parenchyma (Figure 4, G–I). Often, the cytotrophoblast invasion front stopped abruptly a short distance from the implantation site (Figure 4, G–I). Detailed analysis showed that invasive cytotrophoblasts in controls up-regulated CEACAM1, which was strongly associated with the plasma membrane, and expressed cytokeratin in a cytoplasmic pattern (Figure 4, J and L). Many invasive cytotrophoblasts in AD169-infected implants also co-expressed cytokeratin and CEACAM1 (Figure 4K).

Total cytotrophoblast invasion into the renal parenchyma was quantified by measuring the visible area occupied by the implant in sections immunostained for cytokeratin (Figure 4M). The area of invasion in mock-infected controls had a median of 49 relative units and a maximum of 63 relative units. AD169-infected implants were comparable to controls (median, 43 relative units; maximum, 59 relative units). In contrast, VR1814-infected implants showed significantly reduced invasion (median, 13 relative units; maximum, 58 relative units) ($P < 0.05$) relative to control and AD169-infected implants. Titers of virus recovered from infected implants indicated that VR1814 replicated eightfold better than did AD169 and that the laboratory strain failed to yield sufficient virus to detect in three of eight implants. Together, these findings supports and extends the *in vitro* results, showing significant differences between pathogenic and attenuated HCMV strains in the ability to affect the formation of anchoring villi in explants (Figure 1). The results suggested that VR1814 replication in cytotrophoblasts in placental tissue significantly reduced the invasiveness of cells *in vivo* when compared with AD169-infected implants and mock-infected controls.

HCMV Infection Impairs Endovascular Remodeling of Resident Arteries and the Functions of Blood Vessels

During the examination of VR1814- and AD169-infected implants, we observed distinct differences in their appearance under the kidney capsules. Many AD169-infected implants had a network of blood vessels, visible to the naked eye, not seen in any VR1814-infected implants or mock-infected controls. Histological analysis revealed remarkable differences in the vasculature. Control implants had large, cytotrophoblast-remodeled blood vessels in the renal parenchyma (Figure 5, A and B). In striking contrast, VR1814-infected implants had mostly small arteries (Figure 5, C and D), in accord with reduced cytotrophoblast invasiveness (Figure 4, G–I). Like controls, AD169-infected villi had large blood vessels, but these were usually congested (Figure 5, E and F). In some areas, blood leaked into the implant (data not shown), suggesting these remodeled blood vessels were more permeable than those in controls. Vessel diameters in AD169-infected implants averaged 0.25 mm, with many vessel diameters >0.5 mm, whereas those in VR1814-infected implants averaged <0.1 mm. In addition, the cross-sectional areas of blood vessels within implants were quantified by measuring the areas of discernible blood vessels (the five

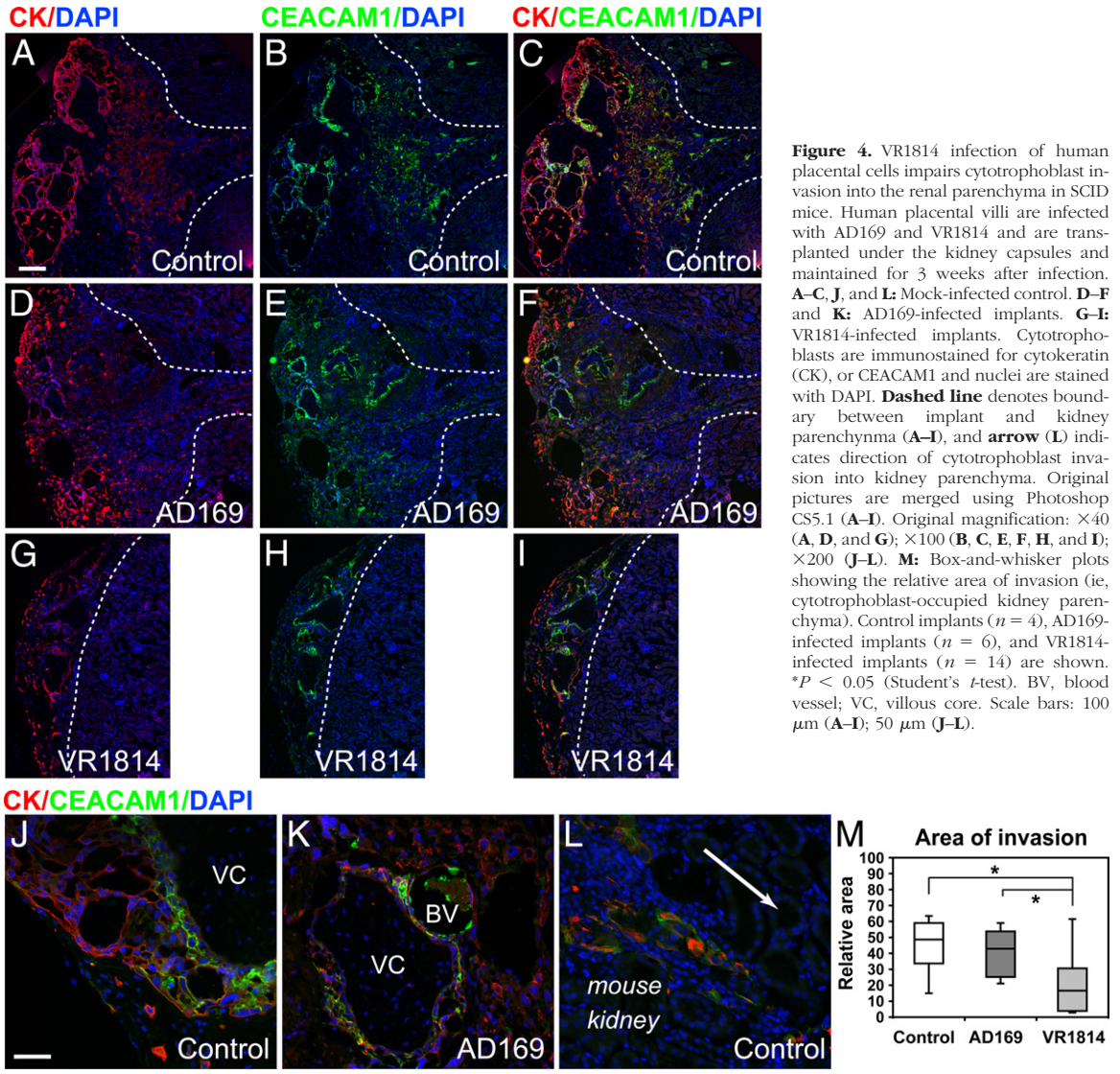

Figure 4. VR1814 infection of human placental cells impairs cytotrophoblast invasion into the renal parenchyma in SCID mice. Human placental villi are infected with AD169 and VR1814 and are transplanted under the kidney capsules and maintained for 3 weeks after infection. **A–C**, **J**, and **L:** Mock-infected control. **D–F** and **K:** AD169-infected implants. **G–I:** VR1814-infected implants. Cytotrophoblasts are immunostained for cytokeratin (CK), or CEACAM1 and nuclei are stained with DAPI. **Dashed line** denotes boundary between implant and kidney parenchynma (**A–I**), and **arrow** (**L**) indicates direction of cytotrophoblast invasion into kidney parenchyma. Original pictures are merged using Photoshop CS5.1 (**A–I**). Original magnification: ×40 (**A**, **D**, and **G**); ×100 (**B**, **C**, **E**, **F**, **H**, and **I**); ×200 (**J–L**). **M:** Box-and-whisker plots showing the relative area of invasion (ie, cytotrophoblast-occupied kidney parenchyma). Control implants ($n = 4$), AD169-infected implants ($n = 6$), and VR1814-infected implants ($n = 14$) are shown. $^{*}P < 0.05$ (Student's *t*-test). BV, blood vessel; VC, villous core. Scale bars: 100 μm (**A–I**); 50 μm (**J–L**).

largest vessels were measured in each case; see *Materials and Methods*). AD169-infected and control implants ($n = 6$ and 4, respectively) had average total cross-sectional areas of 0.20 and 0.26 mm^2, respectively, whereas VR1814-infected implants ($n = 12$) had dramatically lower areas, with an average total area of 0.04 mm^2. Notably, 5 of the 12 VR1814-infected implants had no discernible vessels. Comparison of H&E-stained and adjacent immunostained sections showed that cytokeratin-expressing endovascular cytotrophoblasts had replaced the arterial endothelial cells (Figure 5, G and H). Surprisingly, LYVE-1–expressing lymphatic endothelial cells intercalated between the stretches of endovascular cytotrophoblasts in enlarged blood vessels, suggesting a chimeric vasculature (Figure 5, G and H).

To explore the possibility that differences in remodeling could result in differences in sizes of blood vessels and heterogeneous cellular composition, sections of AD169- and VR1814-infected implants were immunostained for expression of CEACAM1, which is expressed on invasive cytotrophoblasts,[59] and mouse platelet endothelial cell adhesion molecule 1 (CD31), which is expressed on blood vessels. In both implants, endothelial cells expressing platelet endothelial cell adhesion molecule 1 were seen at the periphery and beyond the cytotrophoblast invasion front (Figure 6, A and B). In AD169-infected implants, all large- and moderate-diameter blood vessels were occupied by cytotrophoblasts that expressed CEACAM1 (Figure 6A). In VR1814-infected implants, CEACAM1-expressing cytotrophoblasts were found near villous cores (Figure 6B). Some clustered close to or around or even lined small blood vessels, with little, if any, change in their diameters. Most CEACAM1-expressing blood vessels in AD169-infected implants had larger diameters than those in VR1814-infected implants and suggested remodeling.

Endovascular cytotrophoblasts distinguish between arteries, which they remodel by inducing apoptosis of the endothelial and smooth muscle cells, and veins, with which the cells only superficially interact.[60,61] Differentiating placental cells express ephrins and Eph receptors that enable their interactions with endothelial

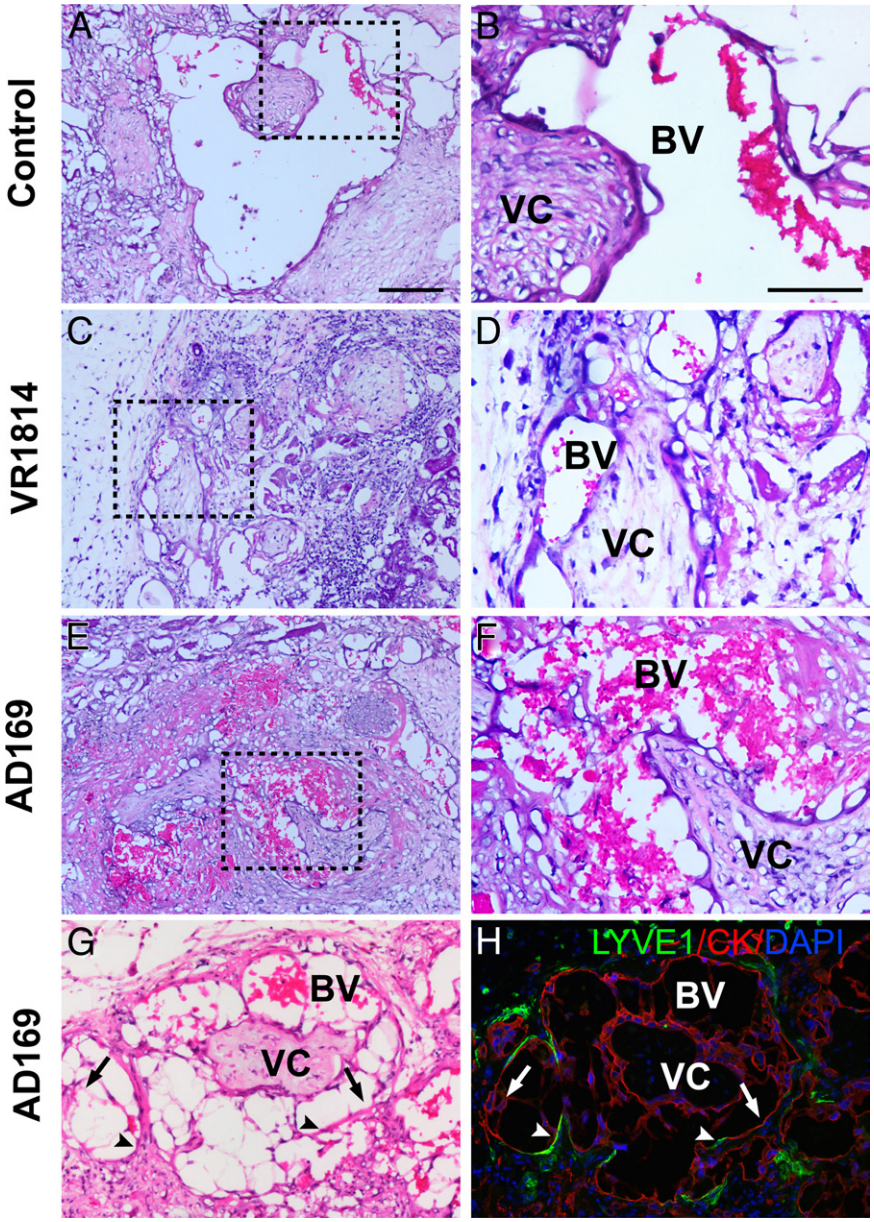

Figure 5. VR1814 infection of human placental cells impairs remodeling of the renal parenchyma in an *in vivo* model of cytotrophoblast invasion in SCID mice. H&E-stained sections of mock-infected control implants [**A** and **B** (magnified from **A**)], VR1814-infected implants [**C** and **D** (magnified from **C**)], and AD169-infected implants [**E** and **F** (magnified from **E**)]. Original magnification: ×100 (**A**, **C**, and **E**); ×200 (**B**, **D**, and **F**). **G:** AD169-infected implants in H&E-stained section show remodeled blood vessels. **Arrows** and **arrowheads** indicate corresponding positions in the adjacent section. **H:** Adjacent section immunostains for cytokeratin (CK) in cytotrophoblasts and LYVE-1 in lymphatic endothelial cells. Original magnification, ×100 in both. BV, blood vessel; VC, villous core. Scale bars: 100 μm (**A**, **C**, **E**, **G**, and **H**); 50 μm (**B**, **D**, and **F**).

cells and contribute to angiogenesis and lymphangiogenesis.[61–63] To test the hypothesis that these molecules could affect migration of cytotrophoblasts *in vivo*, infected implants were immunostained with antibodies to ephrin B2, which selectively marks arteries, cytokeratin, and CEACAM1. An analysis of AD169-infected implants showed a remodeled blood vessel that was largely occupied by cytotrophoblasts that expressed cytokeratin (Figure 6C). Several LYVE-1–positive lymphatic endothelial cells were also present in the vessel wall (Figure 6D). Another blood vessel was even more heterogeneous and contained arterial endothelial cells that expressed ephrin B2 (Figure 6C) surrounded by cytotrophoblasts in the renal parenchyma that expressed cytokeratin and CEACAM1 in blood vessels (Figure 6D). LYVE-1–expressing lymphatic endothelial cells were also assembled into portions of small and large blood vessels (Figure 6D). Detailed analysis of parallel sections revealed that the artery side of this hybrid blood vessel contained endothelial cells that expressed ephrin B2 (Figure 6, E, F, and H). Other areas showed TUNEL staining near endothelial cells (Figure 6, E, G, and H). An immediately adjacent section showed that cytotrophoblasts expressing cytokeratin surrounded the artery (Figure 6I) and clustered near ephrin B2–expressing endothelial cells (Figure 6, I–K) that were positive for TUNEL staining (Figure 6G). Together, the results suggest that cytotrophoblasts in AD169-infected implants induced apoptosis of arterial endothelial cells, the first step in modifying resident arteries. Although apoptosis was not found in arteries when infected implants were examined after 3 weeks *in vivo*, remodeling occurred earlier, and blood vessels containing cytotrophoblasts formed. However, some

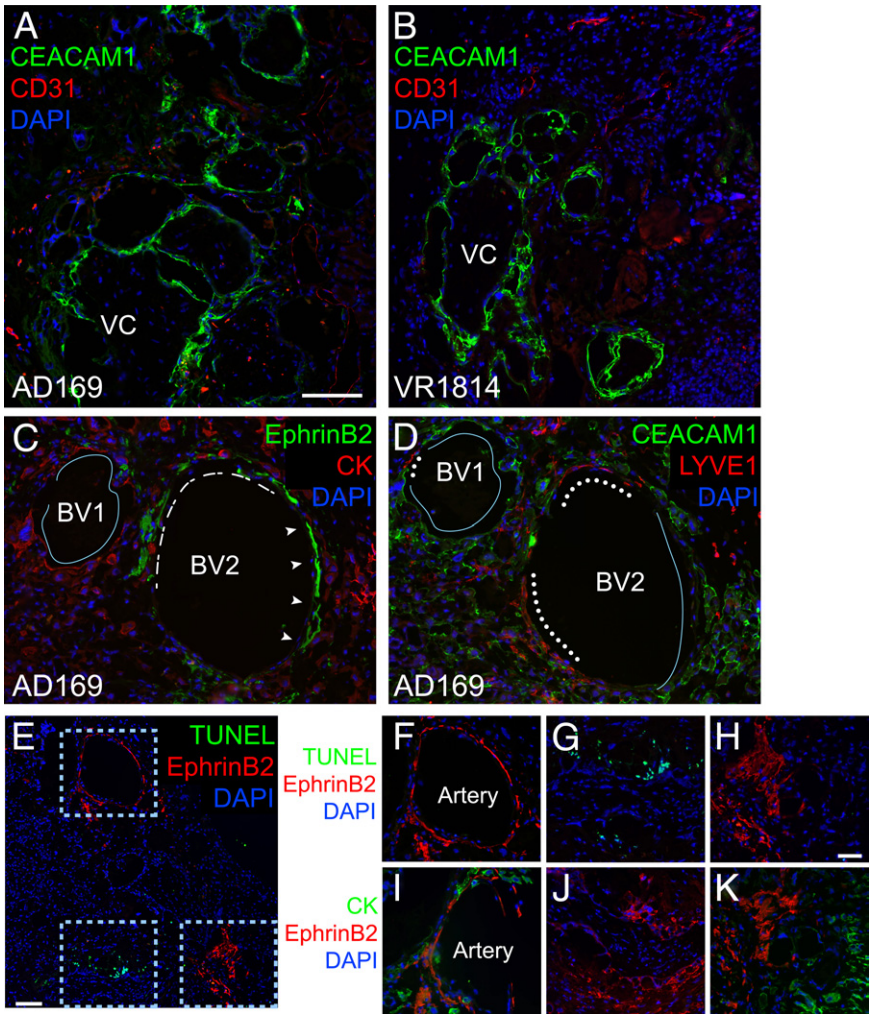

Figure 6. Remodeling of resident arteries defective in AD169-infected placental implants. Human placental villi infected with AD169 or VR1814 are transplanted under the kidney capsules of SCID mice and maintained for 3 weeks. Immunostaining for CEACAM1 and CD31 in AD169-infected (**A**) and VR1814-infected (**B**) implants. Original magnification, ×100. **C** and **D:** Immunostaining for ephrin B2 (**arrowheads**, dashes) and cytokeratin (CK) (line) (**C**) and CEACAM1 (line) and LYVE-1 (dots) (**D**). Original magnification, ×200. **E** and **F–H** (magnified from **E**): Sections adjacent to those in **C** and **D** are evaluated for apoptotic nuclei (green) and immunostained for ephrin B2. **I–K:** Sections adjacent to that in **E** are immunostained for ephrin B2 and CK. Original magnification: ×100 (**E**); ×200 (**F–K**). All sections are counterstained with DAPI to identify nuclei. BV, blood vessel; VC, villous core. Scale bars: 100 μm (**A–D**); 100 μm (**E**); 50 μm (**F–K**).

were chimeras that also contained blood and lymphatic endothelial cells and were congested and permeable to blood, suggesting defective functions.

Infected Primary Cytotrophoblasts and Placental Villous Explants Up-Regulate Expression of Lymphangiogenic Molecules in Vitro

Differentiating cytotrophoblasts express lymphangiogenic molecules[19,64] that promote cell survival and stimulate migration of human lymphatic endothelial cells *in vitro*,[21] including VEGF-A, VEGF-C, and bFGF. In addition, cytotrophoblasts release IL-6, which stimulates angiogenesis and lymphangiogenesis,[65] and AD169 infection increases IL-6 release.[66] In the SCID model of human placentation, we found aberrant lymphangiogenesis in VR1814-infected implants and faulty vascular remodeling in AD169-infected implants, suggesting that these processes could be affected by lymphangiogenic and angiogenic factors. To test this hypothesis, we measured levels of these factors in conditioned media from VR1814- and AD169-infected primary cytotrophoblasts and placental villous explants at 1 and 3 days after infection *in vitro*.

Regarding VEGF-C (Figure 7A), higher levels were produced by VR1814-infected cytotrophoblasts at 1 and 3 days after infection (median, 30.7 and 36.3 pg/mL, respectively) than by AD169-infected cytotrophoblasts (6.9 and 7.3 pg/mL, respectively) or mock-infected controls (0 and 4.5 pg/mL, respectively). In placental villi (Figure 7B), infected and control explants made comparable levels of VEGF-C (control, 20.9 pg/mL; VR1814, 23.8 pg/mL; and AD169, 26.0 pg/mL) at 1 day after infection. At 3 days, VR1814-infected explants tended to make higher levels of VEGF-C (49.7 pg/mL) than did control (36.3 pg/mL) or AD169-infected explants (9 pg/mL). Regarding bFGF (Figure 7C), comparable levels were produced by VR1814-infected (12.7 pg/mL) and AD169-infected (10.0 pg/mL) cytotrophoblasts at 1 day after infection relative to controls (0 pg/mL). At 3 days, although the level for VR1814 remained slightly elevated (7.0 pg/mL), the level for AD169 decreased (0 pg/mL). In placental villi (Figure 7D), much higher bFGF levels were made in VR1814 infection at 1 day after infection (119.2 pg/mL) than in AD169 infection (25.8 pg/mL, $P < 0.05$) or controls (10.9 pg/mL, $P < 0.05$). At 3 days, elevated bFGF levels were maintained in VR1814 infection (71.5 pg/mL, $P < 0.01$ compared with control), and levels in

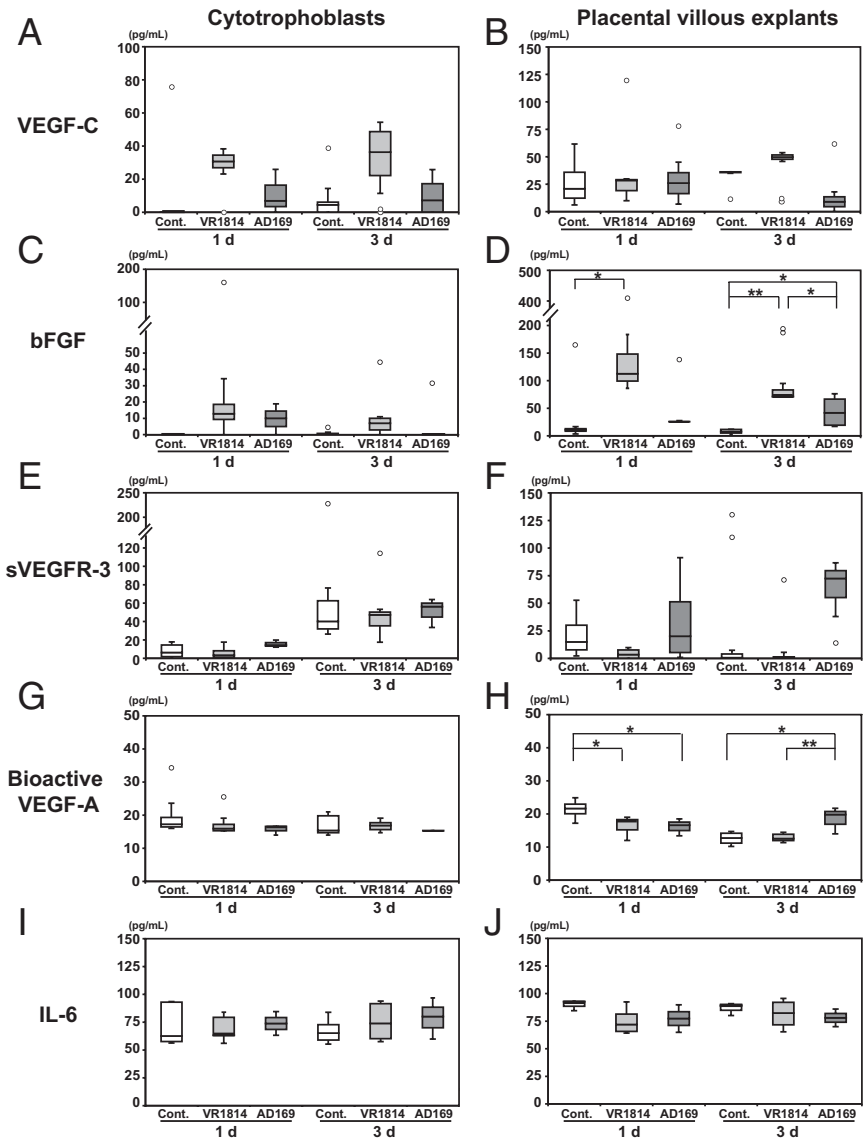

Figure 7. Quantification of cytokines from AD169- and VR1814-infected cytotrophoblasts and placental villous explants *in vitro*. Primary cytotrophoblasts (**A**, **C**, **E**, **G**, and **I**) and placental villous explants (**B**, **D**, **F**, **H**, and **J**) are infected after 12 hours on Matrigel. Conditioned medium is removed at 1 and 3 days (d) after infection, and factors are quantified using ELISA: VEGF-C, bFGF, sVEGFR-3, bioactive VEGF-A, and IL-6. Results are from three to six independent experiments. Cont., control.

AD169 infection increased (41.6 pg/mL, $P < 0.05$ compared with control). Control values were low at both time points (1 day, 10.9 pg/mL; and 3 days, 6.2 pg/mL). Regarding soluble VEGFR-3 (sVEGFR-3; Figure 7E), AD169-infected cytotrophoblasts made more at 1 day after infection (14.3 pg/mL) than did VR1814-infected cells (3.4 pg/mL) or controls (6.3 pg/mL). At 3 days, approximately the same levels of sVEGFR-3 were found in all samples (40.2 to 56.2 pg/mL). In placental villi (Figure 7F), AD169 infection produced high levels of sVEGFR-3 at 1 day (20.1 pg/mL) and even higher levels (72.4 pg/mL) at 3 days, whereas VR1814 infection and controls produced almost no detectable amounts of sVEGFR-3 at 3 days (control, 0.7 pg/mL; VR1814, 0 pg/mL). Regarding bioactive VEGF-A (Figure 7G), infected and control cytotrophoblasts had similarly low levels (14 to 16 pg/mL). In placental villi (Figure 7H), VR1814 and AD169 again made low levels of bioactive VEGF-A (16.0 and 16.6 pg/mL, respectively) compared with controls (21.7 pg/mL) at 1 day ($P < 0.05$). Levels in AD169 infection were higher (19.8 pg/mL) than those in VR1814 infection (12.1 pg/mL, $P < 0.01$) and controls (12.8 pg/mL, $P < 0.05$) at 3 days. Last, regarding IL-6 (Figure 7I), the levels were similar in VR1814-infected and control cytotrophoblasts (control, 62.6 pg/mL at 1 day and 65.2 pg/mL at 3 days; and VR1814, 63.3 pg/mL at 1 day and 73.9 pg/mL at 3 days). Slightly more IL-6 was detected in AD169-infected cytotrophoblasts (73.8 pg/mL at 1 day and 80.1 pg/mL at 3 days). Infected and control cytotrophoblasts (Figure 7J) had comparable levels (63 to 81 pg/mL) at both time points. Likewise, infected and control placental villi (Figure 7J) had comparable levels (72 to 85 pg/mL) at both time points. Together, the results of these experiments indicate that VR1814 infection increases production of VEGF-C and bFGF, whereas AD169 increases bFGF, sVEGFR-3, and bioactive VEGF-A. Interestingly, the differences in levels of cytokines produced by the clinical and laboratory strains were more pronounced in intact placental villi than in primary cytotrophoblasts.

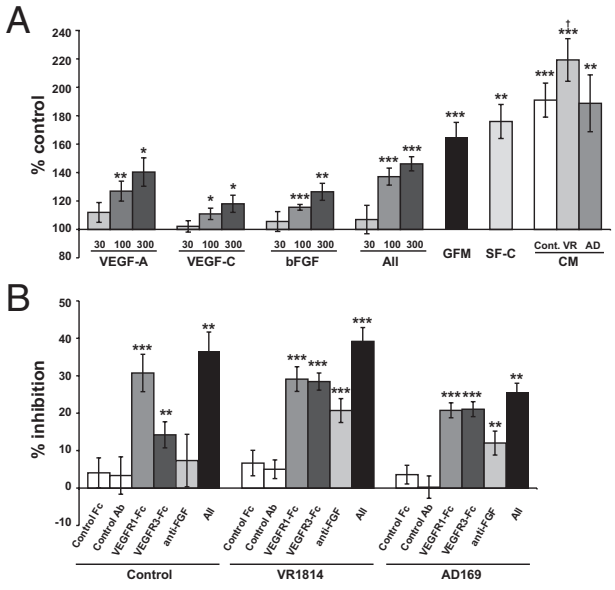

Figure 8. Quantification of lymphatic endothelial cell proliferation *in vitro*. **A:** Lymphatic endothelial cell proliferation assays are performed on cells cultured in media with individual growth factors (30, 100, and 300 ng/mL), all growth factors combined (All; 30, 100, and 300 ng/mL combined, or 10, 33.3, and 100 ng/mL of each), or conditioned media (CM) from control (Cont.) or infected cytotrophoblasts (VR, VR1814; AD, and AD169) collected at 48 hours. Cell proliferation data are expressed as percentages of control values (cells cultured in control media). Experiments (mean ± SE) are performed at least six times in duplicate. $^{*}P < 0.05$, $^{**}P < 0.01$, and $^{***}P < 0.001$ (Student's *t*-test) for comparisons with cells cultured in control media. Data are shown for growth factor medium (GFM), ECM supplemented with endothelial cell growth supplement, and 5% FBS (positive control). $^{\dagger}P < 0.05$ for comparisons with cells cultured in a mixture of serum-free and control media (SF-C). **B:** Blocking effect of VEGFR1-Fc, VEGFR3-Fc, anti-bFGF antibody, and a combination of all three (All) on cell proliferation. Data are expressed as percentages of control values (cells cultured in conditioned medium without inhibitors). Experiments (mean ± SE) are performed at least three times in duplicate. $^{**}P < 0.01$, $^{***}P < 0.001$ (Student's test) for comparisons with cells cultured in conditioned medium alone.

VEGF-A, VEGF-C, and bFGF Stimulate Proliferation of Lymphatic Endothelial Cells

After having found aberrant lymphatic vessel formation and increased numbers of lymphatic endothelial cells in VR1814-infected implants (Figure 3) and differences in the production of lymphangiogenic factors in control and VR1814- and AD169-infected cytotrophoblasts *in vitro* (Figure 7), we investigated whether conditioned medium from VR1814-infected cytotrophoblasts could stimulate lymphatic endothelial cell proliferation *in vitro* using MTT assays. First, HLECs were cultured with recombinant VEGF-A, VEGF-C, or bFGF. Individual growth factors significantly increased cell proliferation in a dose-dependent manner (Figure 8A). A combination of all three growth factors had additive effects on cell proliferation (concentrations in all refer to combined concentrations of all three growth factors; ie, the 300 ng/mL bar represents 100 ng/mL each of the three growth factors, and the additive effect of these can be seen by comparing the 300 ng/mL bar in all with the 100 ng/mL bars in the three individual cases). We then compared the effects of conditioned media from control and VR1814- and AD169-infected cytotrophoblasts on cell proliferation. We found that conditioned medium from VR1814-infected cells significantly promoted cell proliferation relative to SF-C medium. In contrast, conditioned medium from control or AD169-infected cells tended to increase cell proliferation, but this increase was not statistically significant. By using inhibitors that specifically block signaling by VEGF-A (VEGFR1-Fc), VEGF-C (VEGFR3-Fc), and bFGF (anti-bFGF antibody), we determined the relative contributions of these three to the growth-stimulating activities of the various conditioned media. Based on these inhibitor studies, the activity in control conditioned medium was attributed mostly to VEGF-A (Figure 8B). In contrast, in conditioned medium from VR1814-infected cells, the stimulatory activity could be attributed nearly equally to VEGF-A and VEGF-C and, to a lesser extent, bFGF. However, the combination of all three inhibitors did not completely block cell proliferation, suggesting involvement of additional factors.

Pathological Characteristics Associated with Reduced Cytotrophoblast Functions in Congenital HCMV Infection

While studying placentas from pregnancies complicated by congenital HCMV infection, we found evidence of hypoxia resulting from avascular villi and fibrosis, with elevated levels of VEGF-A and a soluble form of its receptor, soluble Flt-1, in amniotic fluid.[14] We considered that the defects observed in HCMV-infected implants in the *in vivo* human placentation model could occur in human pregnancy. In a case of congenital infection with HCMV DNA-positive placental bed biopsy specimens and premature delivery at 31 weeks' gestation, immunostaining for cytokeratin showed that invasive cytotrophoblasts had moderate (Figure 9, A and B) or substantial (Figure 9, C and D) HLA-G down-regulation. In addition, the placental cells exhibited other functional defects. Adjacent to partially remodeled or unmodified blood vessels in decidua, H&E staining showed areas of bleeding and leukocytic infiltration, suggesting inflammation (Figure 9, E and F). This pathological characteristic suggested that differentiating/invading cytotrophoblasts were functionally impaired in remodeling resident uterine arteries.

Discussion

Herein, we studied HCMV pathogenesis in explants of human placental villi infected by a low-passage, endotheliotropic clinical strain and a laboratory strain in a human placentation model of cytotrophoblast-induced arterial remodeling and lymphangiogenesis. By using these techniques, we showed, for the first time to our knowledge, that VR1814 replicates in cytotrophoblasts within the architecture of the human placenta and exhibits pathogenic determinants. Table 1 summarizes HCMV pathogenesis properties identified *in vitro* and *in vivo*. In placental explants, VR1814 replicates in villous and cell column cytotrophoblasts that differentiate into invasive cells and populate anchoring villi. In infected placental

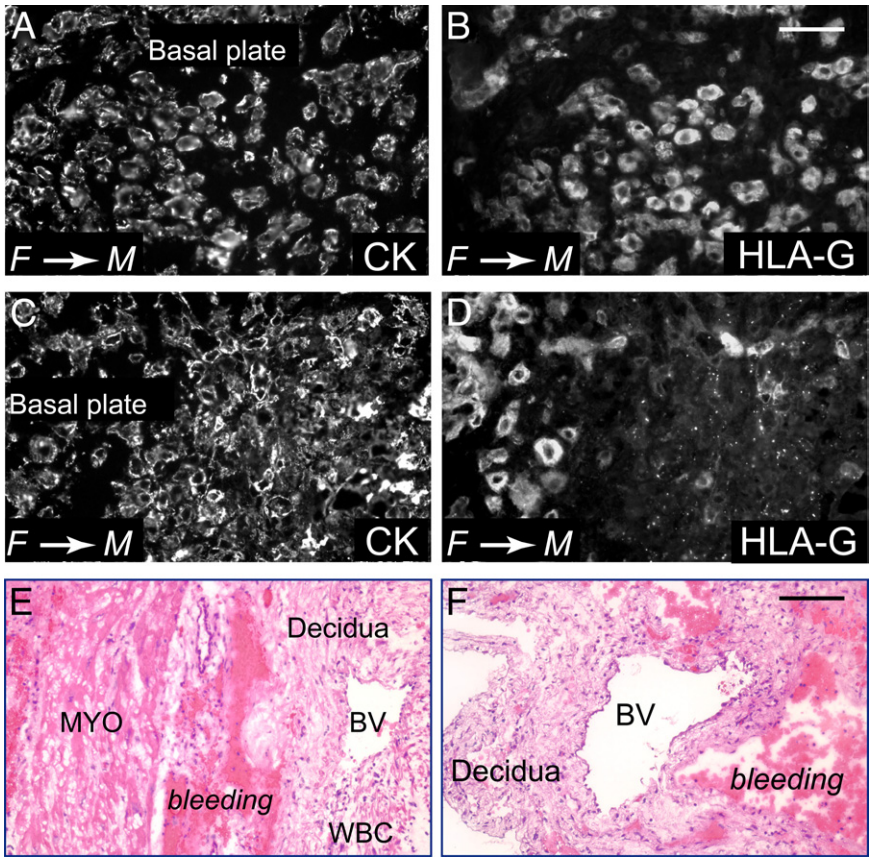

Figure 9. Placental pathological characteristics associated with congenital HCMV infection. Primary maternal infection is identified by seroconversion in a previously HCMV-seronegative woman and low IgG avidity (≤25%) in follow-up tests. **A–F:** Placental bed biopsy specimens from congenital HCMV infection with fetal IUGR at 31 weeks' gestational age. Sections are stained with antibodies to cytokeratin (CK; **A** and **C**) and differentiation molecule MHC class I HLA-G (**B** and **D**) or H&E (**E** and **F**). HLA-G staining of cytotrophoblasts is positive (70%), weakly positive (20%), and negative (10%) in biopsy specimens from the periphery (**B**) and center (**D**) of the placenta. In some sites, HLA-G staining is punctate (**D**). **E** and **F:** Leukocytic infiltration and bleeding near partially modified or unmodified uterine blood vessels (BVs). MYO, myometrium; WBC, white blood cell. F→M, fetal→maternal. Scale bars: 50 μm (**A–D**); 100 μm (**E** and **F**).

xenografts, viral replication dramatically reduced interstitial and endovascular cytotrophoblast invasion and impaired lymphangiogenesis. In striking contrast, AD169 replicates poorly in villous cytotrophoblasts in explants and has negligible effects on the formation of anchoring villi. Likewise, AD169 replication was reduced in human placental xenografts in SCID mice, and cytotrophoblasts differentiated and invaded the kidney parenchyma. Some resident arteries were completely remodeled, whereas others were only partially remodeled. These chimeric blood vessels contained resident arterial endothelial cells, cytotrophoblasts, and lymphatic endothelial cells and were engorged and permeable to blood, suggesting functional defects. VR1814-infected explants significantly increased levels of VEGF-C and bFGF *in vitro*, which could explain abnormal lymphatic endothelial cell proliferation and dysregulated lymphangiogenesis. In contrast, AD169-infected explants substantially increased the level of bioactive VEGF-A, which could promote proliferation of lymphatic endothelial cells and their incorporation into defective blood vessels. Our results suggest that HCMV replication in the placenta enhances the release of paracrine factors that dysregulate cell proliferation and migration and contributes to pathogenesis in the developing placenta.

In congenitally infected placentas, HCMV replicates in several cell types, including uterine glandular epithelial and endothelial cells, decidual cells, and differentiating cytotrophoblasts in the maternal compartment and villous cytotrophoblasts, stromal fibroblasts, and endothelial cells in the fetal compartment.[14,26,38,39,67] Early studies with AD169 showed that the laboratory strain infects primary cytotrophoblasts and down-regulates integrin $\alpha 1\beta 1$ expression, thereby reducing invasiveness *in vitro*.[26] Regarding endotheliotropic clinical strains, VR1814-infected cytotrophoblasts up-regulate cmv IL-10, which decreases matrix metalloproteinase-9 activity, consequently reducing degradation of the extracellular matrix and impeding cell migration.[27] In addition, quantitative analysis showed that VR1814-infected cytotrophoblasts reduce expression of the key integrins and cell-cell adhesion molecules $\alpha 1$, $\alpha 5$, $\alpha 9$, and VE-cadherin, differentiation antigens whose expression is required for pseudovascularization.[18,28,60] Infection in the SCID placentation model shows, for the first time to our knowledge, that invasion defects *in vitro* could affect remodeling of stromal tissue and blood vessels *in vivo*. The diameter of blood vessels and the total area within VR1814-infected implants, indicators of the efficiency of perfusion, were significantly reduced compared with the controls. These results have important implications for the development of IUGR in pregnancies complicated by congenital infection. Together, reduced vascularization, inflammation, and fibrinoid deposition could decrease perfusion of the placental surface, leading to transport defects and hypoxia.[14]

Surprising differences were found in the capacity of the attenuated and low-passage pathogenic strains to infect cytotrophoblasts, replicate, and progress to late infection with gB expression in intact placental villi. All

Table 1. HCMV Pathogenic Features in Infected Human Placental Villi *in Vitro* and *in Vivo*

Strain	Placental villous explants	Placental xenografts in SCID mice
Replication Quantified by Cytotrophoblast Infection and Virus Titers		
VR1814	Infected cytotrophoblasts express gB (median, 30%) (Figure 1, H–K)	Number of infected cytotrophoblasts and virus titers comparable (Figure 2, G and H)
AD169	Cytotrophoblasts infected, but few express gB (median, 2%) (Figure 1, G and K)	Few cytotrophoblasts infected, and virus titers extremely low (data not shown)
Cytotrophoblast Invasion *in Vitro* and Interstitial Invasion of Renal Parenchyma *in Vivo*		
VR1814	Anchoring villi reduced size (Figure 1, C, F, and L)	Cytotrophoblast-occupied area significantly reduced (Figure 4, G–I and M)
AD169	Anchoring villi normal (Figure 1, B, E, and L)	Cytotrophoblast-occupied area comparable to mock-infected controls (Figure 4, D–F and M)
Endovascular Cytotrophoblasts Remodel Resident Arteries *in Vivo*		
VR1814	NA	Resident arteries unmodified (Figure 5, C and D)
AD169	NA	Incompletely remodeled arteries (Figure 6, C and D), congested and permeable to blood (Figure 5, E and F)
Lymphangiogenesis *in Vivo*		
VR1814	NA	LYVE-1–positive lymphatic endothelial cells proliferate, aggregate, and form aberrant vessels (Figure 3, C–E, K, and L)
AD169	NA	LYVE-1–positive lymphatic endothelial cells intercalate with cytotrophoblasts in remodeled blood vessels (Figure 5, G and H, and Figure 6, C and D)
Factors Promoting Cell Proliferation and Lymphangiogenesis Induced *in Vitro* and *in Vivo*		
VR1814	VEGF-C (Figure 7, A and B, and Figure 8) and bFGF (Figures 7D and 8)	Infected cytotrophoblasts up-regulate the expression of VEGF-A and VEGF-C (Figure 3, M and N)
AD169	sVEGFR-3 (Figure 7F), bioactive VEGF-A (Figures 7H and 8), and bFGF (Figures 7D and 8)	ND

NA, not available; ND, no data.

HCMV strains use the conserved core proteins gB and gH/gL, which induce fusion of the virion envelope with the plasma membrane.[34,35] Pathogenic strains express additional proteins, UL128-131A, that form a pentameric complex with gH/gL, facilitating virion attachment and entry into epithelial and endothelial cells.[68–70] In the present study, we showed that AD169 was highly impaired in infection and replication in cell column cytotrophoblasts (Figure 1, B, E, and G). In earlier studies,[33,41] we showed that the strain Toledo infects villous cytotrophoblasts and differentiating/invading cells that express EGFR and integrin $\alpha 1\beta 1$ or $\alpha v\beta 3$, but not cell columns.[33,41] Like clinical HCMV isolates, the strain Toledo carries additional DNA sequences that encode at least 19 genes but have rearrangements of the UL131A gene sequence.[44] Cell columns bridge the gap between the placenta and the uterus and are suspended in the intervillous space by homotypic interactions. They express L-selectin and its carbohydrate ligand, part of a specialized adhesion system activated by shear stress that maintains cell column integrity during the early stages of placental development.[71] This type of adhesion may also facilitate cytotrophoblast movement in and exit from cell columns, a prerequisite for uterine invasion. CEACAM1 mediates homophilic and heterophilic interactions with other adhesion molecules, and its expression in invasive cytotrophoblasts (Figure 4, B, E, H, and J–L, and Figure 6D) suggests that CEACAM1 may also control cytotrophoblast invasion and interactions with the resident vasculature.[59] Regarding the impact of HCMV infection on cell columns, virus replication could decrease the population of cytotrophoblasts capable of progressing further down the differentiation pathway, a prerequisite for interstitial and endovascular invasion. Infection could also perturb the specialized adhesive properties of cell columns, limiting the number of cytotrophoblasts that exit. Together, these events could severely reduce development of anchoring villi in VR1814-infected explants and the cytotrophoblast population capable of invading the in-

terstitium and blood vessels in human placental xenografts.

Uterine spiral artery remodeling involves endothelial apoptosis induced by invasive cytotrophoblasts through Fas/FasL interactions.[21,72] However, pathogenic HCMV strains encode two anti-apoptosis proteins expressed with immediate-early kinetics. In addition to pUL36/vICA, a viral inhibitor of caspase 8–induced apoptosis,[73,74] pUL37, a viral mitochondria-localized inhibitor of apoptosis, protects cells from death induced by a variety of stimuli.[75–79] Abundant expression of pUL36/vICA is detected just a few hours after infection and much earlier than pUL37/viral mitochondria–localized inhibitor of apoptosis, which accumulates later in fibroblasts.[73,74] Coordinate expression of these proteins could maintain survival of infected cells by suppressing apoptosis. Relevant to the results in AD169-infected implants, a mutation in UL36/vICA could delay resistance to Fas-mediated apoptosis.[73] Although not formally tested, it is likely that the anti-apoptotic function was encoded later by pUL37/viral mitochondria-localized inhibitor of apoptosis. After 3 weeks *in vivo*, the functional consequences include partially remodeled blood vessels, some of which still contained resident arterial endothelial cells expressing ephrin B2 (Figure 6, C, E, F, and H–K). The human placentation model enabled realization of the anti-apoptotic determinants in HCMV pathogenesis, for the first time to our knowledge, and provides a framework to test the *in vivo* effects of a mutation in pUL37.

Lymphangiogenic factors have autocrine and paracrine effects that transduce survival and migratory signals in lymphatic endothelial cells[21,80] and maintain cytotrophoblast survival.[19,20] Quantification of factors made in VR1814-infected cytotrophoblasts and explants *in vitro* showed that VEGF-C and bFGF levels were elevated compared with mock-infected controls (Figure 7, A–D). In the model of cytotrophoblast-induced lymphangiogenesis *in vivo*, these factors and others promote migration of lymphatic endothelial cells.[21] In functional experiments, we showed that VEGF-A, VEGF-C, and bFGF each had paracrine effects that increased the proliferation of HLEC and, in combination, had additive effects (Figure 8A). Depletion experiments confirmed the contributions of these factors (Figure 8B). However, failure of the combined inhibitors to completely reduce proliferation indicates the involvement of other factors. Angiogenic factors are essential for the formation of functional vessels and expression in a complementary and coordinated manner to balance stimulatory and inhibitory signals. The increased production of factors that promote lymphatic endothelial cell proliferation in infected cytotrophoblasts could lead to aggregation that precludes formation of a functional lymphatic vasculature (Figure 3, C–G) and could contribute to placental edema in congenital HCMV infection.[13,15,81,82] In AD169 infection, elevated levels of bioactive VEGF-A, which increases blood vessel permeability, and sVEGFR-3 (Figure 7, E–H, and Figure 8B) could reduce vessel function and normal lymphangiogenesis.[83] Moreover, VEGFR-3 antibodies or delivery of sVEGFR-3-Ig fusion protein by an adenovirus vector inhibits angiogenesis by suppressing endothelial sprouting and vascular network formation.[84] Accordingly, dysregulated factors could result in blood vessels composed of both lymphatic endothelial cells and invasive cytotrophoblasts (Figures 5H and 6D). Not previously described, this chimeric vasculature was hyperpermeable to blood, conceivably from incorporation of lymphatic endothelial cells that have junctions specialized for fluid uptake from surrounding tissue.[85] Blood flow could exert pressure on the vessel wall, resulting in leakiness. In contrast to recent reports of a role for elevated IL-6 in HCMV-infected lymphatic endothelial cells in lymphangiogenesis,[65] endothelial cell survival and angiogenesis,[86] and detection of increased IL-6 in AD169-infected trophoblasts immediately after infection,[14] we found no significant increase in AD169- and VR1814-infected cytotrophoblasts and villous explants at either 1 or 3 days (Figure 7, I and J).

Vascular anomalies associated with congenital HCMV infection found in placentas examined at delivery include avascular villi and fibrosis that reduce blood flow to the placental-fetal unit and lead to a condition of intrauterine hypoxia.[12,14] To compensate, placentas increase levels of VEGF-A, which promotes vascular development in the villous core.[12,14] Congenital HCMV infection is associated with 15% of stillbirths and death *in utero* after 20 weeks' gestation, and the placentas have significant thrombotic vasculopathy,[87,88] evidence that links HCMV infection to vascular damage and fetal morbidity.[89] Congenital infection with premature delivery and biopsy specimens with bleeding near partially modified or unmodified uterine blood vessels (Figure 9, E and F) suggest that defective endovascular cytotrophoblast invasion can lead to bleeding in the uterine wall. Other complications of congenital infection include placental edema and fetal hydrops[13,15,81,82] associated with impaired placental development that contributes to IUGR and hypoxia.[90] By using the *in vivo* model of human placentation, we identified dramatic defects in cytotrophoblast differentiation, invasion, and vascular remodeling that could reduce perfusion of the placental surface *in utero*.[26–28] Our results also suggest that paracrine factors could amplify pathology in the decidua by altering lymphangiogenesis, establishing the human placentation model as an experimental system with which to interrogate determinants of viral pathogenesis. We also anticipate that placental explants and xenografts in SCID mice will be invaluable tools for evaluating human monoclonal antibodies with HCMV neutralizing activity as potential treatments that could reduce virus replication and associated pathology in the developing placenta.

Acknowledgments

We thank Mirhan Kapidzic, Matthew Gormley, and Gabriel Goldfein for technical assistance with primary placental cytotrophoblasts and explant cultures, Ekaterina Maidji for early studies on placental xenografts, Cheryl Stoddart for the gift of SCID mice, and Yan Zhou and Susan McDonagh for assistance with analysis of placental biopsy specimens.

References

1. Britt WJ: Congenital Cytomegalovirus Infection. Edited by Hitchcock, PJ MacKay, HT Wasserheit. JN Washington, DC, ASM Press, 1999, pp 269–281
2. Fowler KB, Stagno S, Pass RF: Maternal immunity and prevention of congenital cytomegalovirus infection. JAMA 2003, 289:1008–1011
3. Ross SA, Arora N, Novak Z, Fowler KB, Britt WJ, Boppana SB: Cytomegalovirus reinfections in healthy seroimmune women. J Infect Dis 2010, 201:386–389
4. Demmler GJ: Congenital cytomegalovirus infection and disease. Adv Pediatr Infect Dis 1996, 11:135–162
5. Rivera LB, Boppana SB, Fowler KB, Britt WJ, Stagno S, Pass RF: Predictors of hearing loss in children with symptomatic congenital cytomegalovirus infection. Pediatrics 2002, 110:762–767
6. Pass RF, Stagno S, Myers GJ, Alford CA: Outcome of symptomatic congenital cytomegalovirus infection: results of long-term longitudinal follow-up. Pediatrics 1980, 66:758–762
7. Stagno S, Pass RF, Cloud G, Britt WJ, Henderson RE, Walton PD, Veren DA, Page F, Alford CA: Primary cytomegalovirus infection in pregnancy: incidence, transmission to fetus, and clinical outcome. JAMA 1986, 256:1904–1908
8. Benirschke K, Kaufmann P: Pathology of the Human Placenta. New York, Springer, 2000, pp 616–636
9. Griffiths PD, Baboonian C: A prospective study of primary cytomegalovirus infection during pregnancy: final report. Br J Obstet Gynaecol 1984, 91:307–315
10. Benirschke K, Mendoza GR, Bazeley PL: Placental and fetal manifestations of cytomegalovirus infection. Virchows Arch B Cell Pathol 1974, 16:121–139
11. Monif GR, Dische RM: Viral placentitis in congenital cytomegalovirus infection. Am J Clin Pathol 1972, 58:445–449
12. Garcia AG, Fonseca EF, Marques RL, Lobato YY: Placental morphology in cytomegalovirus infection. Placenta 1989, 10:1–18
13. La Torre R, Nigro G, Mazzocco M, Best AM, Adler SP: Placental enlargement in women with primary maternal cytomegalovirus infection is associated with fetal and neonatal disease. Clin Infect Dis 2006, 43:994–1000
14. Maidji E, Nigro G, Tabata T, McDonagh S, Nozawa N, Shiboski S, Muci S, Anceschi MM, Aziz N, Adler SP, Pereira L: Antibody treatment promotes compensation for human cytomegalovirus-induced pathogenesis and a hypoxia-like condition in placentas with congenital infection. Am J Pathol 2010, 177:1298–1310
15. Rana S, Venkatesha S, DePaepe M, Chien EK, Paglia M, Karumanchi SA: Cyomegalovirus-induced mirror syndrome associated with elevated levels of circulating antiangiogenic factors. Obstet Gynecol 2007, 109(Pt 2):549–552
16. Damsky CH, Fisher SJ: Trophoblast pseudo-vasculogenesis: faking it with endothelial adhesion receptors. Curr Opin Cell Biol 1998, 10: 660–666
17. Damsky CH, Librach C, Lim KH, Fitzgerald ML, McMaster MT, Janatpour M, Zhou Y, Logan SK, Fisher SJ: Integrin switching regulates normal trophoblast invasion. Development 1994, 120:3657–3666
18. Zhou Y, Fisher SJ, Janatpour M, Genbacev O, Dejana E, Wheelock M, Damsky CH: Human cytotrophoblasts adopt a vascular phenotype as they differentiate: a strategy for successful endovascular invasion? J Clin Invest 1997, 99:2139–2151
19. Zhou Y, McMaster M, Woo K, Janatpour M, Perry J, Karpanen T, Alitalo K, Damsky C, Fisher SJ: Vascular endothelial growth factor ligands and receptors that regulate human cytotrophoblast survival are dysregulated in severe preeclampsia and hemolysis, elevated liver enzymes, and low platelets syndrome. Am J Pathol 2002, 160: 1405–1423
20. Zhou Y, Bellingard V, Feng KT, McMaster M, Fisher SJ: Human cytotrophoblasts promote endothelial survival and vascular remodeling through secretion of Ang2, PlGF, and VEGF-C. Dev Biol 2003, 263:114–125
21. Red-Horse K, Rivera J, Schanz A, Zhou Y, Winn V, Kapidzic M, Maltepe E, Okazaki K, Kochman R, Vo KC, Giudice L, Erlebacher A, McCune JM, Stoddart CA, Fisher SJ: Cytotrophoblast induction of arterial apoptosis and lymphangiogenesis in an in vivo model of human placentation. J Clin Invest 2006, 116:2643–2652
22. Kovats S, Main EK, Librach C, Stubblebine M, Fisher SJ, DeMars R: A class I antigen, HLA-G, expressed in human trophoblasts. Science 1990, 248:220–223
23. McMaster MT, Librach CL, Zhou Y, Lim KH, Janatpour MJ, DeMars R, Kovats S, Damsky C, Fisher SJ: Human placental HLA-G expression is restricted to differentiated cytotrophoblasts. J Immunol 1995, 154: 3771–3778
24. Hiby SE, Walker JJ, O'Shaughnessy KM, Redman CW, Carrington M, Trowsdale J, Moffett A: Combinations of maternal KIR and fetal HLA-C genes influence the risk of preeclampsia and reproductive success. J Exp Med 2004, 200:957–965
25. Hiby SE, Apps R, Sharkey AM, Farrell LE, Gardner L, Mulder A, Claas FH, Walker JJ, Redman CW, Morgan L, Tower C, Regan L, Moore GE, Carrington M, Moffett A: Maternal activating KIRs protect against human reproductive failure mediated by fetal HLA-C2. J Clin Invest 2010, 120:4102–4110
26. Fisher S, Genbacev O, Maidji E, Pereira L: Human cytomegalovirus infection of placental cytotrophoblasts in vitro and in utero: implications for transmission and pathogenesis. J Virol 2000, 74:6808–6820
27. Yamamoto-Tabata T, McDonagh S, Chang HT, Fisher S, Pereira L: Human cytomegalovirus interleukin-10 downregulates metalloproteinase activity and impairs endothelial cell migration and placental cytotrophoblast invasiveness in vitro. J Virol 2004, 78:2831–2840
28. Tabata T, McDonagh S, Kawakatsu H, Pereira L: Cytotrophoblasts infected with a pathogenic human cytomegalovirus strain dysregulate cell-matrix and cell-cell adhesion molecules: a quantitative analysis. Placenta 2007, 28:527–537
29. Rauwel B, Mariamé B, Martin H, Nielsen R, Allart S, Pipy B, Mandrup S, Devignes MD, Evain-Brion D, Fournier T, Davrinche C: Activation of peroxisome proliferator-activated receptor gamma by human cytomegalovirus for de novo replication impairs migration and invasiveness of cytotrophoblasts from early placentas. J Virol 2010, 84:2946–2954
30. Fournier T, Guibourdenche J, Handschuh K, Tsatsaris V, Rauwel B, Davrinche C, Evain-Brion D: PPARγ and human trophoblast differentiation. J Reprod Immunol 2011, 90:41–49
31. Simister NE, Story CM, Chen HL, Hunt JS: An IgG-transporting Fc receptor expressed in the syncytiotrophoblast of human placenta. Eur J Immunol 1996, 26:1527–1531
32. Simister NE, Story CM: Human placental Fc receptors and the transmission of antibodies from mother to fetus. J Reprod Immunol 1997, 37:1–23
33. Maidji E, McDonagh S, Genbacev O, Tabata T, Pereira L: Maternal antibodies enhance or prevent cytomegalovirus infection in the placenta by neonatal fc receptor-mediated transcytosis. Am J Pathol 2006, 168:1210–1226
34. Feire AL, Roy RM, Manley K, Compton T: The glycoprotein B disintegrin-like domain binds beta 1 integrin to mediate cytomegalovirus entry. J Virol 2010, 84:10026–10037
35. Feire AL, Koss H, Compton T: Cellular integrins function as entry receptors for human cytomegalovirus via a highly conserved disintegrin-like domain. Proc Natl Acad Sci U S A 2004, 101:15470–15475
36. Wang X, Huong SM, Chiu ML, Raab-Traub N, Huang ES: Epidermal growth factor receptor is a cellular receptor for human cytomegalovirus. Nature 2003, 424:456–461
37. Wang X, Huang DY, Huong SM, Huang ES: Integrin $\alpha v\beta 3$ is a coreceptor for human cytomegalovirus. Nat Med 2005, 11:515–521
38. McDonagh S, Maidji E, Ma W, Chang HT, Fisher S, Pereira L: Viral and bacterial pathogens at the maternal-fetal interface. J Infect Dis 2004, 190:826–834
39. Pereira L, Maidji E, McDonagh S, Genbacev O, Fisher S: Human cytomegalovirus transmission from the uterus to the placenta correlates with the presence of pathogenic bacteria and maternal immunity. J Virol 2003, 77:13301–13314
40. Nozawa N, Fang-Hoover J, Tabata T, Maidji E, Pereira L: Cytomegalovirus-specific, high-avidity IgG with neutralizing activity in maternal circulation enriched in the fetal bloodstream. J Clin Virol 2009, 46(Suppl 4):S58–S63
41. Maidji E, Genbacev O, Chang HT, Pereira L: Developmental regulation of human cytomegalovirus receptors in cytotrophoblasts correlates with distinct replication sites in the placenta. J Virol 2007, 81:4701–4712
42. Mocarski ES, Bonyhadi M, Salimi S, McCune JM, Kaneshima H: Human cytomegalovirus in a SCID-hu mouse: thymic epithelial cells

are prominent targets of viral replication. Proc Natl Acad Sci U S A 1993, 90:104–108
43. Brown JM, Kaneshima H, Mocarski ES: Dramatic interstrain differences in the replication of human cytomegalovirus in SCID-hu mice. J Infect Dis 1995, 171:1599–1603
44. Cha TA, Tom E, Kemble GW, Duke GM, Mocarski ES, Spaete RR: Human cytomegalovirus clinical isolates carry at least 19 genes not found in laboratory strains. J Virol 1996, 70:78–83
45. Wang W, Taylor SL, Leisenfelder SA, Morton R, Moffat JF, Smirnov S, Zhu H: Human cytomegalovirus genes in the 15-kilobase region are required for viral replication in implanted human tissues in SCID mice. J Virol 2005, 79:2115–2123
46. Wang D, Shenk T: Human cytomegalovirus virion protein complex required for epithelial and endothelial cell tropism. Proc Natl Acad Sci U S A 2005, 102:18153–18158
47. Schuessler A, Sampaio KL, Straschewski S, Sinzger C: Mutational mapping of pUL131A of human cytomegalovirus emphasizes its central role for endothelial cell tropism. J Virol 2012, 86:504–512
48. Baldanti F, Paolucci S, Campanini G, Sarasini A, Percivalle E, Revello MG, Gerna G: Human cytomegalovirus UL131A, UL130 and UL128 genes are highly conserved among field isolates. Arch Virol 2006, 151:1225–1233
49. Gerna G, Sarasini A, Patrone M, Percivalle E, Fiorina L, Campanini G, Gallina A, Baldanti F, Revello MG: Human cytomegalovirus serum neutralizing antibodies block virus infection of endothelial/epithelial cells, but not fibroblasts, early during primary infection. J Gen Virol 2008, 89:853–865
50. Macagno A, Bernasconi NL, Vanzetta F, Dander E, Sarasini A, Revello MG, Gerna G, Sallusto F, Lanzavecchia A: Isolation of human monoclonal antibodies that potently neutralize human cytomegalovirus infection by targeting different epitopes on the gH/gL/UL128-131A complex. J Virol 2010, 84:1005–1013
51. Revello MG, Baldanti F, Percivalle E, Sarasini A, De-Giuli L, Genini E, Lilleri D, Labo N, Gerna G: In vitro selection of human cytomegalovirus variants unable to transfer virus and virus products from infected cells to polymorphonuclear leukocytes and to grow in endothelial cells. J Gen Virol 2001, 82:1429–1438
52. Librach CL, Werb Z, Fitzgerald ML, Chiu K, Corwin NM, Esteves RA, Grobelny D, Galardy R, Damsky CH, Fisher SJ: 92-kD type IV collagenase mediates invasion of human cytotrophoblasts. J Cell Biol 1991, 113:437–449
53. McCune JM, Namikawa R, Kaneshima H, Shultz LD, Lieberman M, Weissman IL: The SCID-hu mouse: murine model for the analysis of human hematolymphoid differentiation and function. Science 1988, 241:1632–1639
54. Dondero DV, Pereira L: Monoclonal Antibody Production. Edited by Emmons, R Schmidt. N Washington, DC, American Public Health Association, 1990, pp 101–124
55. Pereira L, Hoffman M, Tatsuno M, Dondero D: Polymorphism of human cytomegalovirus glycoproteins characterized by monoclonal antibodies. Virology 1984, 139:73–86
56. Chen C, Kudo M, Rutaganira F, Takano H, Lee C, Atakilit A, Robinett KS, Uede T, Wolters P, Shokat K, Huang X, Sheppard D: Integrin $\alpha 9\beta 1$ in airway smooth muscle suppresses exaggerated airway narrowing. J Clin Invest 2012, 122:2916–2927
57. Sylvester PW: Optimization of the Tetrazolium Dye (MTT) Colorimetric Assay for Cellular Growth and Viability. Drug Design and Discovery: Methods and Protocols (Methods in Molecular Biology). Edited by S Satyanarayanajois. New York, Humana Press, 2011, Vol. 716, pp 157–168
58. Lee HW, Qin YX, Kim YM, Park EY, Hwang JS, Huo GH, Yang CW, Kim WY, Kim J: Expression of lymphatic endothelium-specific hyaluronan receptor LYVE-1 in the developing mouse kidney. Cell Tissue Res 2011, 343:429–444
59. Bamberger AM, Sudahl S, Loning T, Wagener C, Bamberger CM, Drakakis P, Coutifaris C, Makrigiannakis A: The adhesion molecule CEACAM1 (CD66a, C-CAM, BGP) is specifically expressed by the extravillous intermediate trophoblast. Am J Pathol 2000, 156:1165–1170
60. Zhou Y, Damsky CH, Fisher SJ: Preeclampsia is associated with failure of human cytotrophoblasts to mimic a vascular adhesion phenotype: one cause of defective endovascular invasion in this syndrome? J Clin Invest 1997, 99:2152–2164
61. Red-Horse K, Kapidzic M, Zhou Y, Feng KT, Singh H, Fisher SJ: EPHB4 regulates chemokine-evoked trophoblast responses: a mechanism for incorporating the human placenta into the maternal circulation. Development 2005, 132:4097–4106
62. Wang HU, Chen ZF, Anderson DJ: Molecular distinction and angiogenic interaction between embryonic arteries and veins revealed by ephrin-B2 and its receptor Eph-B4. Cell 1998, 93:741–753
63. Wang Y, Nakayama M, Pitulescu ME, Schmidt TS, Bochenek ML, Sakakibara A, Adams S, Davy A, Deutsch U, Luthi U, Barberis A, Benjamin LE, Makinen T, Nobes CD, Adams RH: Ephrin-B2 controls VEGF-induced angiogenesis and lymphangiogenesis. Nature 2010, 465:483–486
64. Zhou Y, Genbacev O, Fisher SJ: The human placenta remodels the uterus by using a combination of molecules that govern vasculogenesis or leukocyte extravasation. Ann N Y Acad Sci 2003, 995:73–83
65. Fiorentini S, Luganini A, Dell'oste V, Lorusso B, Cervi E, Caccuri F, Bonardelli S, Landolfo S, Caruso A, Gribaudo G: Human cytomegalovirus productively infects lymphatic endothelial cells and induces a secretome that promotes angiogenesis and lymphangiogenesis through interleukin-6 and granulocyte-macrophage colony-stimulating factor. J Gen Virol 2010, 92:650–660
66. Halwachs-Baumann G, Weihrauch G, Gruber HJ, Desoye G, Sinzger C: hCMV induced IL-6 release in trophoblast and trophoblast like cells. J Clin Virol 2006, 37:91–97
67. McDonagh S, Maidji E, Chang HT, Pereira L: Patterns of human cytomegalovirus infection in term placentas: a preliminary analysis. J Clin Virol 2006, 35:210–215
68. Wang D, Shenk T: Human cytomegalovirus UL131 open reading frame is required for epithelial cell tropism. J Virol 2005, 79:10330–10338
69. Scrivano L, Sinzger C, Nitschko H, Koszinowski UH, Adler B: HCMV spread and cell tropism are determined by distinct virus populations. PLoS Pathog 2011, 7:e1001256
70. Adler B, Scrivano L, Ruzcics Z, Rupp B, Sinzger C, Koszinowski U: Role of human cytomegalovirus UL131A in cell type-specific virus entry and release. J Gen Virol 2006, 87:2451–2460
71. Prakobphol A, Genbacev O, Gormley M, Kapidzic M, Fisher SJ: A role for the L-selectin adhesion system in mediating cytotrophoblast emigration from the placenta. Dev Biol 2006, 298:107–117
72. Ashton SV, Whitley GS, Dash PR, Wareing M, Crocker IP, Baker PN, Cartwright JE: Uterine spiral artery remodeling involves endothelial apoptosis induced by extravillous trophoblasts through Fas/FasL interactions. Arterioscler Thromb Vasc Biol 2005, 25:102–108
73. Skaletskaya A, Bartle LM, Chittenden T, McCormick AL, Mocarski ES, Goldmacher VS: A cytomegalovirus-encoded inhibitor of apoptosis that suppresses caspase-8 activation. Proc Natl Acad Sci U S A 2001, 98:7829–7834
74. Patterson CE, Shenk T: Human cytomegalovirus UL36 protein is dispensable for viral replication in cultured cells. J Virol 1999, 73: 7126–7131
75. Goldmacher VS, Bartle LM, Skaletskaya A, Dionne CA, Kedersha NL, Vater CA, Han J, Lutz RJ, Watanabe S, McFarland ED, Kieff ED, Mocarski ES, Chittenden T: A cytomegalovirus-encoded mitochondria-localized inhibitor of apoptosis structurally unrelated to Bcl-2. Proc Natl Acad Sci U S A 1999, 96:12536–12541
76. McCormick AL, Skaletskaya A, Barry PA, Mocarski ES, Goldmacher VS: Differential function and expression of the viral inhibitor of caspase 8-induced apoptosis (vICA) and the viral mitochondria-localized inhibitor of apoptosis (vMIA) cell death suppressors conserved in primate and rodent cytomegaloviruses. Virology 2003, 316:221–233
77. McCormick AL, Smith VL, Chow D, Mocarski ES: Disruption of mitochondrial networks by the human cytomegalovirus UL37 gene product viral mitochondrion-localized inhibitor of apoptosis. J Virol 2003, 77:631–641
78. Reboredo M, Greaves RF, Hahn G: Human cytomegalovirus proteins encoded by UL37 exon 1 protect infected fibroblasts against virus-induced apoptosis and are required for efficient virus replication. J Gen Virol 2004, 85:3555–3567
79. Sharon-Friling R, Goodhouse J, Colberg-Poley AM, Shenk T: Human cytomegalovirus pUL37x1 induces the release of endoplasmic reticulum calcium stores. Proc Natl Acad Sci U S A 2006, 103:19117–19122
80. Makinen T, Veikkola T, Mustjoki S, Karpanen T, Catimel B, Nice EC, Wise L, Mercer A, Kowalski H, Kerjaschki D, Stacker SA, Achen MG, Alitalo K: Isolated lymphatic endothelial cells transduce growth, survival and migratory signals via the VEGF-C/D receptor VEGFR-3. EMBO J 2001, 20:4762–4773

81. Sampath V, Narendran V, Donovan EF, Stanek J, Schleiss MR: Non-immune hydrops fetalis and fulminant fatal disease due to congenital cytomegalovirus infection in a premature infant. J Perinatol 2005, 25:608–611
82. Barron SD, Pass RF: Infectious causes of hydrops fetalis. Semin Perinatol 1995, 19:493–501
83. Makinen T, Jussila L, Veikkola T, Karpanen T, Kettunen MI, Pulkkanen KJ, Kauppinen R, Jackson DG, Kubo H, Nishikawa S, Yla-Herttuala S, Alitalo K: Inhibition of lymphangiogenesis with resulting lymphedema in transgenic mice expressing soluble VEGF receptor-3. Nat Med 2001, 7:199–205
84. Tammela T, Zarkada G, Wallgard E, Murtomaki A, Suchting S, Wirzenius M, Waltari M, Hellstrom M, Schomber T, Peltonen R, Freitas C, Duarte A, Isoniemi H, Laakkonen P, Christofori G, Yla-Herttuala S, Shibuya M, Pytowski B, Eichmann A, Betsholtz C, Alitalo K: Blocking VEGFR-3 suppresses angiogenic sprouting and vascular network formation. Nature 2008, 454:656–660
85. Baluk P, Fuxe J, Hashizume H, Romano T, Lashnits E, Butz S, Vestweber D, Corada M, Molendini C, Dejana E, McDonald DM: Functionally specialized junctions between endothelial cells of lymphatic vessels. J Exp Med 2007, 204:2349–2362
86. Botto S, Streblow DN, DeFilippis V, White L, Kreklywich CN, Smith PP, Caposio P: IL-6 in human cytomegalovirus secretome promotes angiogenesis and survival of endothelial cells through the stimulation of survivin. Blood 2011, 117:352–361
87. Syridou G, Spanakis N, Konstantinidou A, Piperaki ET, Kafetzis D, Patsouris E, Antsaklis A, Tsakris A: Detection of cytomegalovirus, parvovirus B19 and herpes simplex viruses in cases of intrauterine fetal death: association with pathological findings. J Med Virol 2008, 80:1776–1782
88. Iwasenko JM, Howard J, Arbuckle S, Graf N, Hall B, Craig ME, Rawlinson WD: Human cytomegalovirus infection is detected frequently in stillbirths and is associated with fetal thrombotic vasculopathy. J Infect Dis 2011, 203:1526–1533
89. Pereira L: Have we overlooked congenital cytomegalovirus infection as a cause of stillbirth? J Infect Dis 2011, 203:1510–1512
90. Noyola DE, Demmler GJ, Nelson CT, Griesser C, Williamson WD, Atkins JT, Rozelle J, Turcich M, Llorente AM, Sellers-Vinson S, Reynolds A, Bale JF Jr, Gerson P, Yow MD: Early predictors of neurodevelopmental outcome in symptomatic congenital cytomegalovirus infection. J Pediatr 2001, 138:325–331